JOURNAL OF NEUROPHYSIOLOGY
Vol. 72, No. 4, October 1994. *Printed in U.S.A.*

Neural Responses Related to Smooth-Pursuit Eye Movements and Their Correspondence With Electrically Elicited Smooth Eye Movements in the Primate Frontal Eye Field

JACQUELINE P. GOTTLIEB, MARTHA G. MACAVOY, AND CHARLES J. BRUCE
Yale University School of Medicine, Section of Neurobiology, New Haven, Connecticut 06510

SUMMARY AND CONCLUSIONS

1. Intracortical microstimulation of a portion of the monkey frontal eye field (FEF) lying in the floor and posterior bank of the arcuate sulcus evokes smooth, rather than saccadic eye movements. To further explore this region's involvement in pursuit, we recorded from FEF neurons in the vicinity of sites from which smooth eye movements (SEMs) were elicited electrically and studied their responses during smooth-pursuit and saccadic tasks. In this report, we describe the neurons' responses during visually guided smooth pursuit and compare their locations and response properties with those of elicited SEMs.

2. One hundred and ninety-three neurons, recorded from the FEF region in six hemispheres of three rhesus monkeys, were classified as "pursuit neurons". These neurons responded during smooth-pursuit tracking of moving visual stimuli but had no, or only minimal, responses in conjunction with visually guided saccades. Pursuit neurons were located in a small region of the arcuate fundus and posterior bank that overlapped, and extended slightly beyond, the region from which SEMs were elicited with microstimulation.

3. All pursuit neurons had a preferred pursuit direction, and all directions were represented with no strong bias toward ipsilateral, contralateral, up, or down. The directional tuning of 80 pursuit cells was measured quantitatively by testing pursuit in several directions and fitting the responses to a Gaussian function. Tuning indices (the σ parameter of the Gaussian fit) varied between 13° and 136°. The median tuning index, 44.5°, corresponds to a full width at half maximum of 105°. The ubiquity of selectivity for pursuit direction and the wide distribution of preferred directions indicates that pursuit direction uses a place-code type of representation in FEF; however, the broad directional tuning of most neurons suggests that pursuit direction is given by a weighted average of optimal directions across the population of pursuit neurons active at any given time.

4. In general, the responses of pursuit neurons increased with pursuit velocity. Of 13 neurons formally tested with 2 s of constant-velocity tracking in their preferred direction across a range of target speeds, pursuit velocity sensitivity ranged from 0.24 to 1.42 spikes $\cdot s^{-1} \cdot deg^{-1} \cdot s^{-1}$, with an average sensitivity of 0.70. This relationship suggests that pursuit neurons represent pursuit magnitude using a rate code; this parallels our previous observation that at most SEM sites, the velocity and acceleration of the electrically elicited eye movements increased as a function of the stimulation current.

5. Pursuit responses began at a median latency of 103 ms (n = 69) after target motion began. When latencies were computed relative to the initiation of smooth pursuit, the majority (61%) discharged before pursuit in their preferred direction and the median relative latency was −19 ms (with negative meaning that the discharge preceded pursuit). Thus significant FEF activity could contribute to the early stages of pursuit initiation, consistent with the previous observation that FEF stimulation elicits SEMs from stationary fixation.

6. We recorded pursuit responses and subsequently tested microstimulation at 113 sites. Of these, the electrical stimulation yielded SEMs at 27, saccades at 12, and no eye movements at the remaining 74 sites. The response latencies of neurons at SEM sites did not differ from those at sites yielding no elicited eye movements; however, SEMs were elicited more often from sites where neurons preferred pursuit directed ipsilateral to the recording hemisphere, relative to those with contralateral preferred directions.

7. The direction of elicited SEMs were correlated with the best tracking direction of neurons recorded at the SEM site (r_+ = 0.71). Despite this highly significant overall correlation, however, elicited SEM direction varied by ~40°, on average, from the best pursuit direction of the neuron. This discrepancy may reflect the broad directional tuning of pursuit neurons and the relatively large currents, 50–100 μA, that were often used to obtain these elicited SEMs.

8. The correspondence between the location and direction preferences of pursuit neurons and those of elicited SEMs, as well as the short latencies of the pursuit responses, suggest that FEF pursuit neurons participate in the generation of pursuit eye movements and that microstimulation of this region elicits SEMs by activating these pursuit neurons, and hence their projections to other parts of the smooth pursuit system.

INTRODUCTION

A large number of behavioral and physiological studies have implicated the primate frontal eye field (FEF) in the generation of saccades—eye movements specialized for rapid capture of targets of interest (for reviews see Bruce 1990; Goldberg and Segraves 1989). However, recent experiments have shown that the FEF also contributes to the control of smooth-pursuit eye movements, a distinct class of voluntary eye movements specialized for tracking moving visual targets. Experimental FEF lesions can compromise pursuit gain as well as the ability to track predictively (in anticipation of, rather than in response to target motion) (Keating 1991, 1993; Lynch 1987; MacAvoy et al. 1991). Additionally, we (Gottlieb et al. 1993; MacAvoy et al. 1991) have shown that low-intensity microstimulation in a circumscribed region of the monkey FEF elicits slow, continuous eye movements (SEMs) that are quite distinct from the rapid, discrete eye movements electrically elicited from the saccadic FEF. These elicited SEMs are predominantly ipsilateral in direction, in agreement with the principally ipsilateral nature of pursuit deficits caused by unilat-

eral lesions of both the monkey and human FEF (MacAvoy et al. 1991; Morrow and Sharpe 1990; but see Keating 1991). Moreover, the location of this SEM region—in the fundus of the arcuate sulcus and neighboring posterior bank—is consistent with the observations that only FEF lesions involving the arcuate fundus produce pursuit deficits, whereas lesions confined to the anterior arcuate bank and lip leave pursuit intact (Keating 1993; MacAvoy et al. 1991).

To further investigate the FEF contributions to pursuit, we recorded neuronal activity in the vicinity of SEM sites. We find that many neurons in this SEM sector of the arcuate respond during smooth pursuit, but not in relation to saccadic eye movements, and that the best tracking direction of such pursuit neurons generally matches the direction of SEMs elicited from their site. Moreover, most pursuit neurons start responding before the start of the pursuit movement, consistent with the previous observation that FEF stimulation readily elicits SEMs from stationary fixation and suggesting that FEF could contribute to both the initiation and maintenance of pursuit and hence be an integral part of neocortical circuitry for smooth pursuit.

Preliminary reports of these data have appeared previously (Gottlieb et al. 1989, 1991; MacAvoy et al. 1991).

METHODS

Surgery and animal care

Three adult female rhesus monkeys (*Macaca mulatta*) were prepared for chronic single-neuron recording and microstimulation in aseptic surgical procedures under sodium pentobarbital anesthesia. A search coil for monitoring eye movements (3 turns of Teflon-coated stainless steel wire) was implanted under the conjunctivum of one eye using standard methods (Judge et al. 1980). A craniotomy (2 cm diam) was trephined over the right frontal lobe, and a stainless steel recording chamber was placed over the craniotomy. To secure the implant, stainless steel bolts with flattened heads were run along slots in the skull with the bolt head under the skull and secured with nuts above the skull. The chamber, bolts, connector for the search coil, and a steel receptacle for attaching the monkey's head to the monkey chair were bound together with dental acrylic. Analgesics [pentazocine lactate, 5 mg/kg im or oral acetaminophen (Tylenol)] were given postoperatively as indicated. After several months of recording in the right hemisphere, a recording cylinder was placed over the left frontal lobe in a shorter additional surgery.

During the course of the physiology experiments, the monkeys obtained liquid to satiety each day by performing oculomotor tasks and had restricted access to water in their home cages. The experimental and surgical protocols were approved by the Yale University Animal Care and Use Committee and complied with United States Public Health Service policy on the humane care and use of laboratory animals.

Physiological methods

Eye position was recorded using the search coil method (Robinson 1963). The field coil, power oscillator, and phase detectors were made by CNC Engineering (Seattle, WA). The search coil signals were calibrated while the monkey fixated small lights at different locations. Horizontal and vertical eye position signals and their differentiated counterparts, horizontal and vertical eye velocity traces, were sampled by the computer every 2 ms.

Single units were recorded with glass-coated Elgiloy electrodes having tip exposures of 20–50 μm and in vivo impedances of 0.5–2 MΩ at 1 kHz, or glass-coated Tungsten electrodes with tip exposures of 10–20 μm and impedances of 0.5–1 MΩ at 1 kHz. The microelectrode signals were amplified by $\times$10 using a preamplifier close to the monkey and subsequently low-pass filtered at 10 kHz and high-pass filtered at 200 Hz to eliminate 60-kHz coil driver artifact, 60-Hz noise, and slow DC shifts. Signals were monitored on a digital oscilloscope, and a time/amplitude-window discriminator (DIS-1, BAK Electronics) was used to recognize action potentials and provide acceptance pulses to the computer.

After the study of most cells, we tested for electrically elicited eye movements as described later.

Behavioral tasks

During experimental sessions, the monkeys sat in a primate chair with their heads restrained, facing a gray tangent screen 57 cm distant. Experiments were conducted either with low-level background illumination or in complete darkness (except for the visual targets). Visual targets (red lights, 0.5° diam) were back-projected and moved on this screen by a *X-Y* mirror system (General Scanning). The monkeys were trained to fixate or follow these lights, and their oculomotor behavior was monitored using a position (fixation) window centered on the target. A PDP-11 computer (DEC) presented and moved the visual targets, stored the neuronal spike times and eye movement traces, and rewarded correct behavior with drops (0.1 ml) of fruit drink.

The data presented here were obtained in several tasks.

SMOOTH PURSUIT TASKS. The monkey initiated each trial by achieving and maintaining fixation of a stationary target for a variable interval (0.9–1.3 s). After this initial epoch, the fixation target began to move, and the monkey was required to track it closely to receive rewards. Target motion could be either constant velocity (CV), with velocities of 2.5–50°/s and durations of 0.75–2 s, or sinusoidal, with peak-to-peak amplitudes of 20–40°, frequencies of 0.25–1.25 Hz, and a duration of 2–3 cycles. The target's direction and velocity (or sinusoidal amplitude) were determined on each trial either through an experimenter-manipulated joystick ("interactive tasks") or by a coordinate array specified at the beginning of the experiment, whose members were tested in pseudorandom order.

Generally the initial fixation position was located opposite the impending target motion with its eccentricity such that the total target excursion was symmetrical about the center of the screen. However, in a *step-ramp* variant of the CV pursuit task, the target always first appeared at the center of the screen and, after being fixated by the monkey, jumped to an eccentric location (the step) and instantaneously began moving with constant velocity (the ramp). Thus the step determined the retinal locus of the initial visual stimulation, whereas the ramp determined the direction and speed of pursuit.

VISUALLY GUIDED SACCADE TASK. The initially central fixation target jumped to a peripheral location and remained visible and stationary. The monkey was rewarded for reacquiring the target with an appropriate saccade of reasonable latency (e.g., $\leq$500 ms).

MICROSTIMULATION TASKS. Intracortical microstimulation was tested during attentive fixation using 75- to 500-ms trains of biphasic (negative-positive) pulses (0.2-ms duration, 25–100 μA, 300 Hz) delivered through the recording electrode. After the monkey had fixated a stationary target light for a variable interval (0.5–1.75 s), the stimulation train was gated by the computer. The fixation requirement was relaxed during the stimulation so that the monkey was not penalized for elicited movements; however, the monkey was required to reacquire the target after the end of the stimulation train and fixate for an additional 0.25–0.5 s before obtaining a reward. In a *stimulation-and-stabilization* variant, the fixation light was stabilized electronically on the fovea for the

duration of the stimulation train, thus eliminating the retinal slip caused by an elicited eye movement in the presence of a stationary target. For further details regarding these microstimulation tasks and parameters, see Gottlieb et al. (1993).

Sampling of cortical sites

Electrodes were introduced through the intact dura and advanced through the cortex using a Narishige hydraulic microdrive system. In *monkeys HN* and *DN*, electrodes were positioned relative to the millimeter grid affixed to the drive stage. In *monkey HZ*, we introduced the grid system made by Crist Instrument (Crist et al. 1988). In this system, a plastic grid with 1-mm spacing between holes along each orthogonal axis determined the brain surface coordinates, and the electrode was advanced into the cortex through a guide tube (a fine-gauge stainless steel hypodermic tube) introduced into the grid at the desired coordinates at the beginning of each recording session. This arrangement reduced the variability in electrode paths arising from different electrode bends and penetration angles and improved the accuracy and reproducibility of penetrations, especially at sites deep in the arcuate sulcus.

Histological techniques

Selected sites were marked either by iron deposits (10–14 μA of positive current for 2–3 min through the Elgiloy electrodes) or by electrolytic lesions (20 μA of negative current for 30 s) made with both types of electrode. At the completion of the experiments, each monkey received an overdose of sodium pentobarbital and was perfused transcardially with saline followed by a 1.25% glutaraldehyde-1.0% paraformaldehyde mixture. The brains were sectioned at 40 μm on a freezing microtome. The brain of *monkey DN* was sectioned in the coronal plane; each hemisphere of *monkeys HZ* and *HN* was sectioned approximately perpendicular to the arcuate sulcus at its caudal limit, a plane more appropriate for visualizing the sulcal cortex. Every second or third section through the arcuate sulcus region was reacted with ferrocyanide (Perl's reaction) for visibility of the iron deposits, then counterstained with neutral red or cresyl violet. Outlines of the lateral aspect of the frontal cortex were reconstructed from drawings of selected histological sections. The locations of electrode penetrations were reconstructed with reference to histologically identified penetrations.

Data acquisition and analysis

Data were stored in two types of computer records. *Analog record* files contained the horizontal and vertical components of stimulus position, eye position, and eye velocity sampled each 4 ms during tracking trials together with corresponding unit spikes. *Unit buffer* files contained the time of occurrence of each spike and also events that could be used as triggers for response histograms. Possible triggers included any computer-controlled event, such as the appearance or disappearance of visual stimuli, the beginning or ending of stimulus motion, and the four movement phases of sinusoidal motion cycles (0, 90, 180, and 270°). In addition, histograms could be triggered on oculomotor events such as the beginning or ending of saccades of specified dimensions or the achieving or leaving of a fixation window.

Response magnitude for CV tasks was estimated typically by averaging the activity over the entire duration of target motion. For sinusoidal tasks, a partial Fourier transform of the activity over the entire duration of target motion was first computed to obtain the average rate (F_0), and the amplitude (F_1), and phase shift at the frequency being tested. Response magnitude then was estimated as the sum of the F_0 and F_1 components of this decomposition. Error trials in which the monkeys' gaze exited the fixation window always were excluded from the histograms used to obtained these response-magnitude numbers.

For quantitative testing of a cell's directional preference, response magnitude during pursuit of four to eight different directions were fit to the Gaussian function $f(d) = B + R\, e^{-0.5(|d-\phi|/\sigma)^2}$ where $f(d)$ is discharge rate at a given direction (d), B represents the background rate and can either be the cell's true baseline firing or an estimate provided by the fitting algorithm, ϕ is an estimate of the cell's best direction, and R estimates the cell's response at its best direction. σ is an index of tuning width, equal to the distance from best direction, $|d - \phi|$, for which the cell responds at 60%, ($e^{-1/2}$) of its maximal response above baseline. The fit was implemented by finding the combination of parameters B, R, ϕ, and σ that minimized the least squared errors using the Levenberg-Marquardt method. The covariance matrix at the estimated parameter values provided a standard error for each estimate, which was used to compute 95% confidence intervals for the estimates. To compare the tuning index σ to other reports, we also computed the distance z at which the Gaussian curve is half of its maximal response above baseline. The formula is $z = \sigma\sqrt{(2 \ln 2)} = 1.177\ \sigma$, and thus the full width of the tuning curve at half-maximal response (2 z) is $2.354 \times \sigma$.

As described in RESULTS, this Gaussian fit of directional tuning was obtained for 80 pursuit cells. On average, these fits were based on 6.9 different pursuit directions, with the majority being based on 8 different pursuit directions; however, for 21 cells, this fit was based on only 4 directions. For these fits, we used the fixed parameter B at the cell's baseline rate so that the number of data points (4) still exceeded the number of parameters being fit (3). The σ (tuning index) obtained from these cells is probably less accurate than estimates of σ obtained with a larger set of data, but omitting these 21 cells changed the median σ by <1°. Likewise, the ϕ (best direction) obtained from fitting only 4 directions is probably less accurate than those obtained with 8 directions, but nevertheless these estimates of ϕ generally confirmed the interactive estimates of the unit's best direction.

To quantify the SEMs elicited by microstimulation, horizontal and vertical smooth eye velocity traces were generated by removing any saccades and interpolating eye velocity through the saccade. The polar direction and velocity of the elicited SEM was computed in each trial from the horizontal and vertical smooth eye velocity components, and the median polar direction of the elicited SEM then was calculated from blocks of 5–15 trials with identical stimulation conditions (see Gottlieb et al. 1993 for further details).

RESULTS

FEF pursuit neurons

Neurons in the FEF region of frontal cortex were classified as "pursuit neurons" if they responded during smooth pursuit of moving visual targets, but did not respond, or responded only minimally, in relation to saccadic eye movements or to fixation of stationary targets. Furthermore, we required that pursuit neurons be directionally selective, and that they have excitatory responses for pursuit in their preferred direction. Figure 1 shows responses of a representative pursuit neuron with a preferred tracking direction of down and slightly right (polar 290°). During CV tracking along its preferred direction (*bottom left*), the neuron began responding ~100 ms after the light began to move and discharged tonically throughout the remaining excursion. The neuron was silent during CV tracking in the opposite direction (110°), having only a small, transient response after extinction of the target at the end of that excursion.

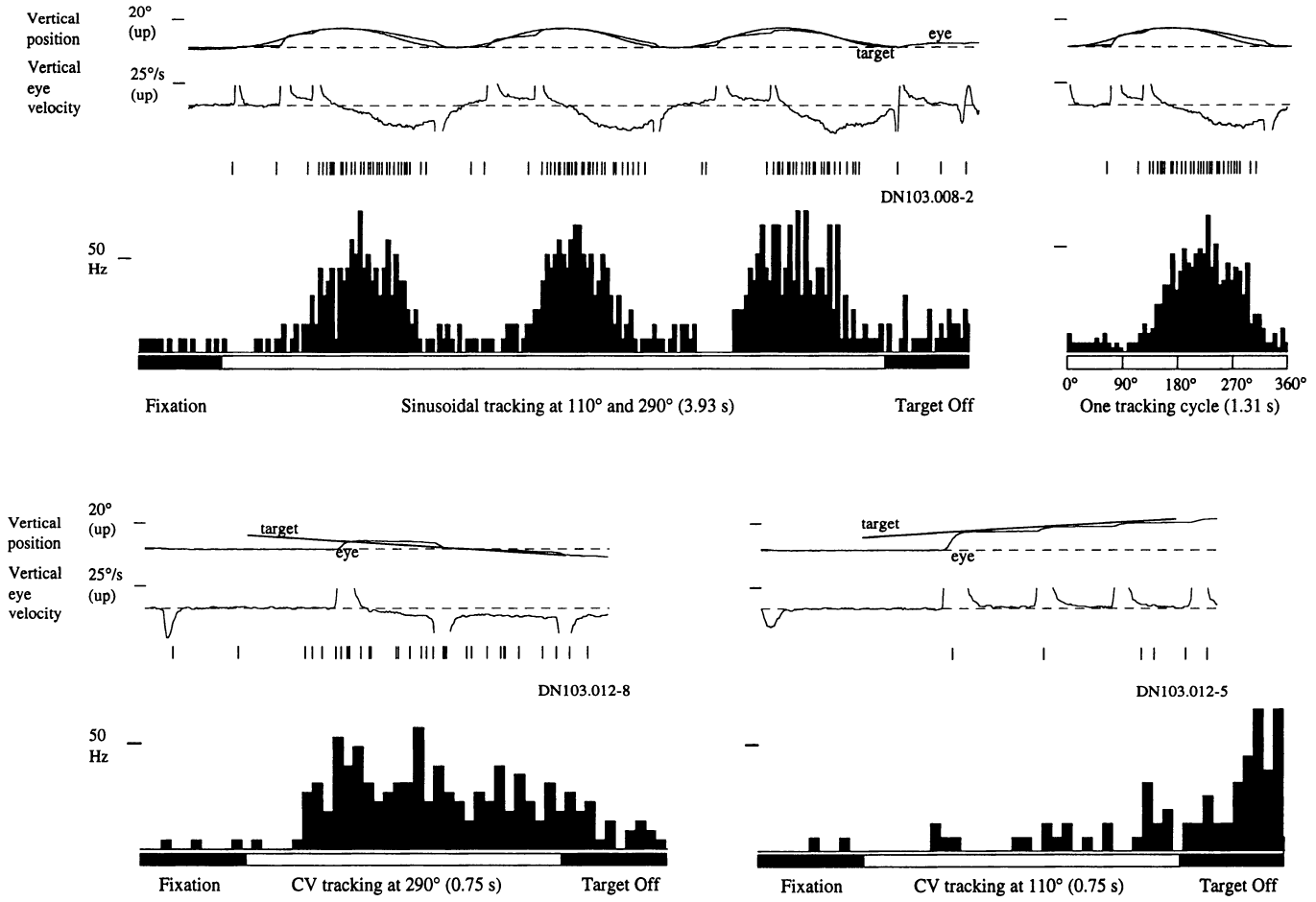

FIG. 1. Pursuit responses of a frontal eye field (FEF) neuron (*DN103*, right hemisphere). Responses during tracking sinusoidal motion (*top*), with 0.762-Hz frequency and 15° peak-to-peak amplitude, directed along the 110–290° axis. Only the vertical components of the eye traces are shown because this motion is principally up and down. The histogram (*left*) is averaged from 6 trials and aligned on the beginning of target motion in each trial; the other (*right*) shows the same responses aligned by phase on each movement cycle (average of 18 cycles). Notice that the neuron's response profile is approximately sinusoidal, slightly leading the 180° phase (corresponding with the onset of motion in its preferred direction) and peaking before the 270° phase (corresponding with the peak target velocity in its preferred direction). Same neuron's responses (*bottom*) during constant-velocity tracking directed at 290° (*left*) and 110° (*right*). Target speed was 20°/s, and the 10° steps were opposite the cell's preferred pursuit direction (110°) in both conditions. In these and all subsequent eye records, upward deflections represent rightward or upward movements and downward deflections indicate leftward or downward movements. The time scales for each histogram and corresponding eye records are given by open bars indicating the tracking epoch. Bin widths for these and all subsequent histograms are 20 ms unless otherwise indicated. Note the lack of correlation, in the single records, between the neural activity and the saccades made during tracking. Also note the lack of response during stationary fixation.

During sinusoidal tracking, the neuron responded in phase with the target motion, with its peak response occurring after the onset of target motion in its preferred direction (corresponding with the 180° phase on the figure), but before the target reached its maximal velocity in that direction (corresponding with the 270° phase). As is evident in the histograms, the cell did not respond during fixation of the stationary light prior to target motion. Furthermore as seen in the single-trial records, these responses were not related to the saccades the monkey made during tracking. In other testing (not shown), the neuron was unresponsive when the visually guided saccade task was used to elicit small downward saccades similar to the catch-up saccades that often occurred during tracking in its preferred direction.

Thus on the basis of its responses on the standard pursuit and saccade tasks described above, the cell of Fig. 1 satisfied our definition of a pursuit cell. Altogether, we recorded 193 such pursuit neurons in the FEF regions of the six hemispheres of the three rhesus monkeys. In this report, we describe these neurons' responses during smooth pursuit including their direction and speed preferences, their response latencies relative to stimulus events and eye movements, and the correspondence between their preferred pursuit directions and the directions of SEMs electrically elicited at their sites.

For many of these pursuit cells, we also performed additional control experiments to dissect their functional activities. In Fig. 2 we show an example of such control experiments for the purpose of demonstrating that these FEF pursuit responses cannot be accounted for trivially by a single, isolated sensory or motor aspect of the pursuit situation, such as the stimulation of a discrete, motion-selective visual receptive field by the pursuit target or the modulation of a sensitivity to eye position within the orbit by the pursuit

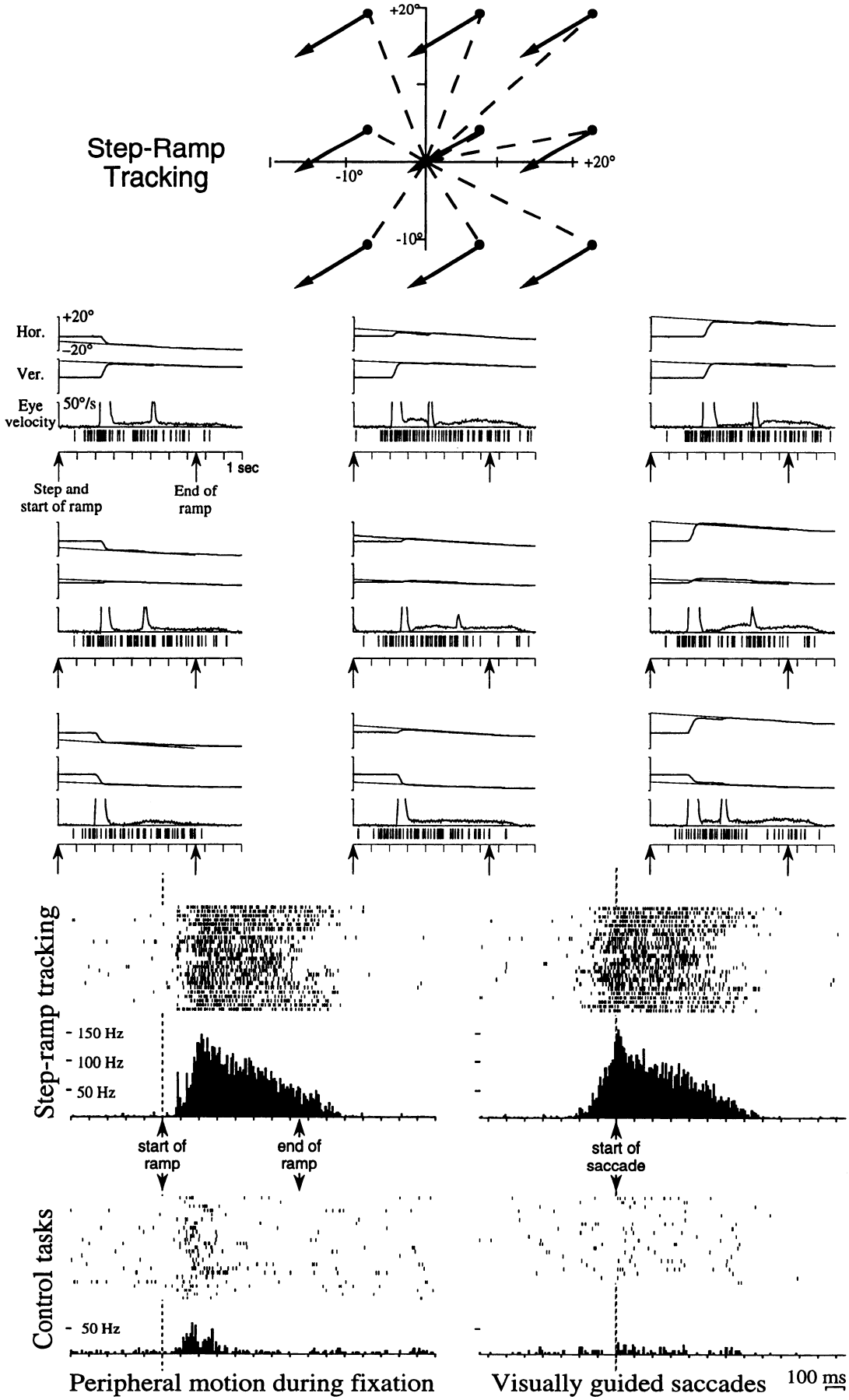
Step-Ramp Tracking
+20°
-10°
+20°
-10°
Hor.
Ver.
Eye velocity
50°/s
1 sec
Step and start of ramp
End of ramp
Step-ramp tracking
150 Hz
100 Hz
50 Hz
start of ramp
end of ramp
start of saccade
Control tasks
50 Hz
Peripheral motion during fixation
Visually guided saccades
100 ms

excursion. For the cell of Fig. 2, which preferred pursuit to the left and down (~210° polar; see also Fig. 12), we arranged the step-ramp experiment diagrammed in the *top* of the figure. After the monkey achieved fixation at the screen center, the target jumped (the step) to one of nine different sectors of the screen and immediately began moving (the ramp) at 15°/s in the cell's preferred direction. The monkey typically made a saccade to reacquire the target with a latency of 200–300 ms after the step and then tracked the ramp motion with smooth pursuit aided by a few small catch-up saccades. The monkey made no presaccadic smooth pursuit as described by Rashbass (1961); however, it usually had achieved a significant smooth velocity by the end of the first saccade.

RETINAL SLIP. The pursuit-related responses of this cell (shown in the single-trial records and the step-ramp histograms of Fig. 2) cannot exclusively reflect stimulation of a motion-selective visual receptive field by the retinal slip of the pursuit target. The visual motion control experiment (Fig. 2, *bottom left*) used the same nine step-ramp coordinates; however, the central light was not extinguished and the monkey was required maintain its fixation and thus not pursue the peripheral moving stimuli. Although this cell, like most pursuit cells, did respond to such peripheral visual motion tested during continued fixation, its response in the step-ramp task was far stronger and more long lasting. We measured neural responses in a 100-ms interval starting 90 ms after the peripheral motion began; because saccade latencies were usually >200 ms, these neural responses reflect the same peripheral retinal stimulation in both tasks. The average discharge in the visual motion control task was 34 Hz versus 59 Hz in the step-ramp tracking task. The discharge disparity in the next 100-ms interval was even greater as the visual motion rate fell to 24 Hz, whereas the tracking rate rose to 128 Hz; this interval should still reflect fairly identical peripheral motion across the two tasks when the neural response latency as well as the eye-movement latency is considered. Finally, as is evident in the records of this cell and of most other cells shown in this paper, pursuit responses usually continued long after the monkey had greatly reduced the target's retinal slip by achieving a smooth-pursuit velocity that roughly matched the target velocity. In this example, the tracking response remained fairly high, being 65 Hz in the last 100 ms of the tracking period. In contrast, there was no discernible response in the last 100 ms of the visual motion stimulation period, the discharge rate having dropped to the cell's baseline (~2 Hz). Note that this absence of response cannot simply reflect the moving stimulus leaving a discrete visual receptive field because in the pursuit situation, the cell not only responded for targets moving near the fovea but also for targets moving in the upper, lower, left, and right visual fields as shown by the step-ramp experiment.

BACKGROUND VISUAL MOTION. Because this cell responded well before the smooth-pursuit eye movement began, its responses could not simply reflect stimulation by the opposing motion of the visual background that is brought about by the pursuit movement itself. As documented below, most FEF pursuit cells responded before pursuit eye movements began. Furthermore all pursuit cells tested while tracking a target light in otherwise complete darkness (n = 12) had responses comparable with their responses during pursuit with standard dim background illumination.

EYE VELOCITY. The fact that pursuit responses began well before the onset of the smooth eye movement (see also the section on response latencies) also argues against pursuit activity simply being a corollary discharge derived from smooth eye velocity signals in the brain stem. Moreover, as already mentioned, most pursuit cells also had some responses to peripheral visual motion tested during fixation of a stationary light.

ORBITAL POSITION. The step-ramp responses of the neuron in Fig. 2 also demonstrate that traversing a particular range of eye positions is not critical because the cell's discharge continued following saccades that brought the eye to quite different orbital sectors. Furthermore there was no response to roughly the same set of saccades made during the saccade-only control (Fig. 2, *bottom right*). Conversely within a particular orbital path, the response critically depended on the pursuit direction; this was verified in all pursuit cells by testing tracking along the same path but in opposite directions, as can be seen in Figs. 1, 3, and 12. Thus pursuit cells are not simply those FEF cells that are sensitive to the

FIG. 2. Activity of a pursuit neuron (*DN303*, left hemisphere) that responded in conjunction with smooth pursuit directed to the left and down. A step-ramp experiment (*top*) with 9 different steps with the same ramp (speed: 15°/sec, direction: 210° polar) is depicted. Step movements (- - -) are shown from the center to where the small black spots are located and arrows represent the subsequent ramp movements lasting 750 ms (excursion 11°). Nine records (*middle*) show target motion and eye movements (H, V), eye velocity (e), and neuronal activity (tics below the eye velocity trace) for a representative trial associated with each of the 9 steps. Each record begins at the step and lasts 1 s, thus including the 750-ms ramp and 250 ms after the target disappeared. For all 9 steps, the cell began responding before the initial saccade and continued to respond while the monkey tracked the ramp. Notice that smooth pursuit typically did not begin until during or after the initial saccade. Raster histograms (*bottom*) showing the cell's activity on all trials of the step-ramp task and on matching control tasks. Cell (*bottom left*) responded much more on the step-ramp task (*above*) than in a visual motion control task (*below*) employing the same ramp motion starting at the same 9 peripheral locations. In this control task, the central light remained on and the monkey was required to maintain central fixation and not track the peripheral targets. Raster histograms are aligned on the onset of peripheral target motion; the histogram sums all trials correctly performed (56 step-ramp, 27 control), and the rasters show the first 25 such trials for both tasks (for trials 7–15 of the step-ramp task the ramp duration was temporarily shortened to 500 ms to encourage the monkey—note the shortened discharge period in the corresponding raster lines). Cell responded very little (*bottom right*) in a visually guided saccade paradigm using the same 9 steps as used in the step-ramp task, but with the targets remaining stationary (0 ramp velocity) after the steps. Here the raster histogram is aligned on the start of the saccadic eye movements, the histogram sums all correctly performed trials, and the raster shows all 22 such trials in this control task. Fig. 12 has additional data of this cell and shows the smooth eye movements that were obtained by microstimulation at the site of this cell.

position of the eye in the orbit (Bizzi 1968; Bruce and Goldberg 1985; Schall 1991). Even though some pursuit neurons were clearly modulated by orbital position during stationary fixation and/or during tracking, we judged this orbital effect to be in addition to, rather than the cause of, their pursuit responses.

In summary, the discharges of these FEF cells in conjunction with smooth-pursuit tracking are not trivially related to a single sensory or motor factor. However, the factors discussed above are related to pursuit performance and, as we will describe in a subsequent report, most do have significant correlations with or effects upon the activity of FEF pursuit neurons.

Directional selectivity of pursuit responses

Each neuron's "best tracking direction" (the direction eliciting the strongest response) was estimated initially in an interactive task wherein pursuit direction was varied from trial-to-trial using an experimenter-controlled joystick. For 80 neurons, directional tuning was studied further quantitatively by measuring responses during tracking in four to eight different directions flanking the neuron's interactively estimated best direction, and then fitting a Gaussian function of direction to these responses (see METHODS). Such a formal direction test of one neuron is shown in Fig. 3. This cell responded strongly during upward tracking, especially at 90° and 135°, and was inhibited during downward tracking, especially at 270° and 315°. The Gaussian fit of its tracking responses indicated a best direction (ϕ) of 106° with a 95% confidence interval of (103°, 109°) and a tuning index (σ) of 46°. Like many other pursuit neurons, including the one in Fig. 1, this cell also was excited transiently after the end of tracking in its off direction and transiently inhibited after on-direction tracking.

Figure 4 shows the directional tuning data and Gaussian curve fits for five additional pursuit neurons. As illustrated in this figure, responses of different pursuit cells ranged from narrowly tuned (σ = 13°) to broadly tuned (σ = 136°). The median σ was 44.5° (n = 80), which translates to an average full width at half-maximal response of 104.75° (see METHODS for the conversion formula) and indicates that the directional selectivity of pursuit cells was generally broad.

Figure 5 shows the best pursuit directions of all 193 pursuit neurons, including the 80 that were estimated by the Gaussian fits and the remaining 113 whose directions were only estimated by the experimenter using the interactive task. Directions of left hemisphere neurons were mirror reversed to allow grouping of all data points as "contralateral" or "ipsilateral". Notice that all possible directions appear to be represented, with no apparent bias toward horizontal or vertical, nor toward contralateral or ipsilateral pursuit.

Latencies of pursuit responses

Response latency relative to the start of target movement was measured from cumulative histograms averaged across several CV tracking trials (typically 5–10) in a neuron's preferred direction. Neurons that were tested exclusively with sinusoidal tasks, in which the gradual buildup of target velocity was likely to complicate identification of latencies, as well as neurons with high baseline rates or with unclear response onsets, were not included in this analysis. Neuron response latencies relative to the start of target motion ranged from 28 to 352 ms (n = 69), with a median of 103 ms.

To determine whether these neurons could participate in pursuit initiation, we compared each neuron's latency relative to target motion with the average pursuit eye movement latency on the same sets of trials. This comparison is illustrated in Fig. 6 for four neurons. For each neuron are shown individual response rasters, cumulative response histograms, and averaged smooth eye velocity traces (saccades were removed from these traces before averaging). Neurons A–C began responding, respectively, at 71, 70, and 104 ms after target motion began, and led pursuit initiation by 90, 48, and 21 ms. Neuron D began responding 125 ms after target motion began and lagged pursuit initiation by 10 ms.

The latency difference distribution for all 69 neurons is shown in Fig. 7. Neural activity led pursuit initiation for 42 (61%) neurons and started only after the smooth-pursuit movement began for the remaining 27 neurons, with the overall median latency difference being −19 ms (negative signifies that the neural discharge leads the pursuit). Thus most FEF pursuit neurons could contribute to early stages of pursuit initiation and almost all could contribute to late stages of pursuit initiation.

The idea that different neurons participate in different stages of pursuit processing also is supported by observations of the neural response profiles during CV tracking. Thus some neurons responded best before and during the start of pursuit, which is characterized by high retinal slip and eye accelerations, suggesting that they contribute preferentially to pursuit initiation (e.g., the neuron in Figs. 2 and 12). Others had tonic response profiles and thus could contribute both to pursuit initiation and maintenance (e.g., the neuron in Fig. 3).

Velocity sensitivity

High tracking velocities were usually not needed to elicit robust neural responses; however, most neurons responded more in conjunction with faster pursuit. Figure 8 shows one neuron's responses and the corresponding sets of eye movements during tracking of target ramps at speeds ranging from 2.5 to 25°/s. This neuron had tonic responses that clearly increased in parallel with the increases in target and eye velocity.

Response rates of this and of three additional neurons as functions of pursuit velocity are plotted in Fig. 9 and fit with regression lines. For this analysis, the average spiking rate and the average pursuit velocity over the 2-s tracking interval was computed for each trial. For 13 neurons formally tested, including the 4 shown in Fig. 9, spike rate was significantly correlated with pursuit velocity ($P < 0.05$; one-tailed). Velocity sensitivities (the slopes of the linear regression fits) ranged from 0.24 to 1.42, with an average sensitivity of 0.70 spikes $\cdot s^{-1} \cdot deg^{-1} \cdot s^{-1}$. Responses of an additional neuron tested for sensitivity to pursuit velocity

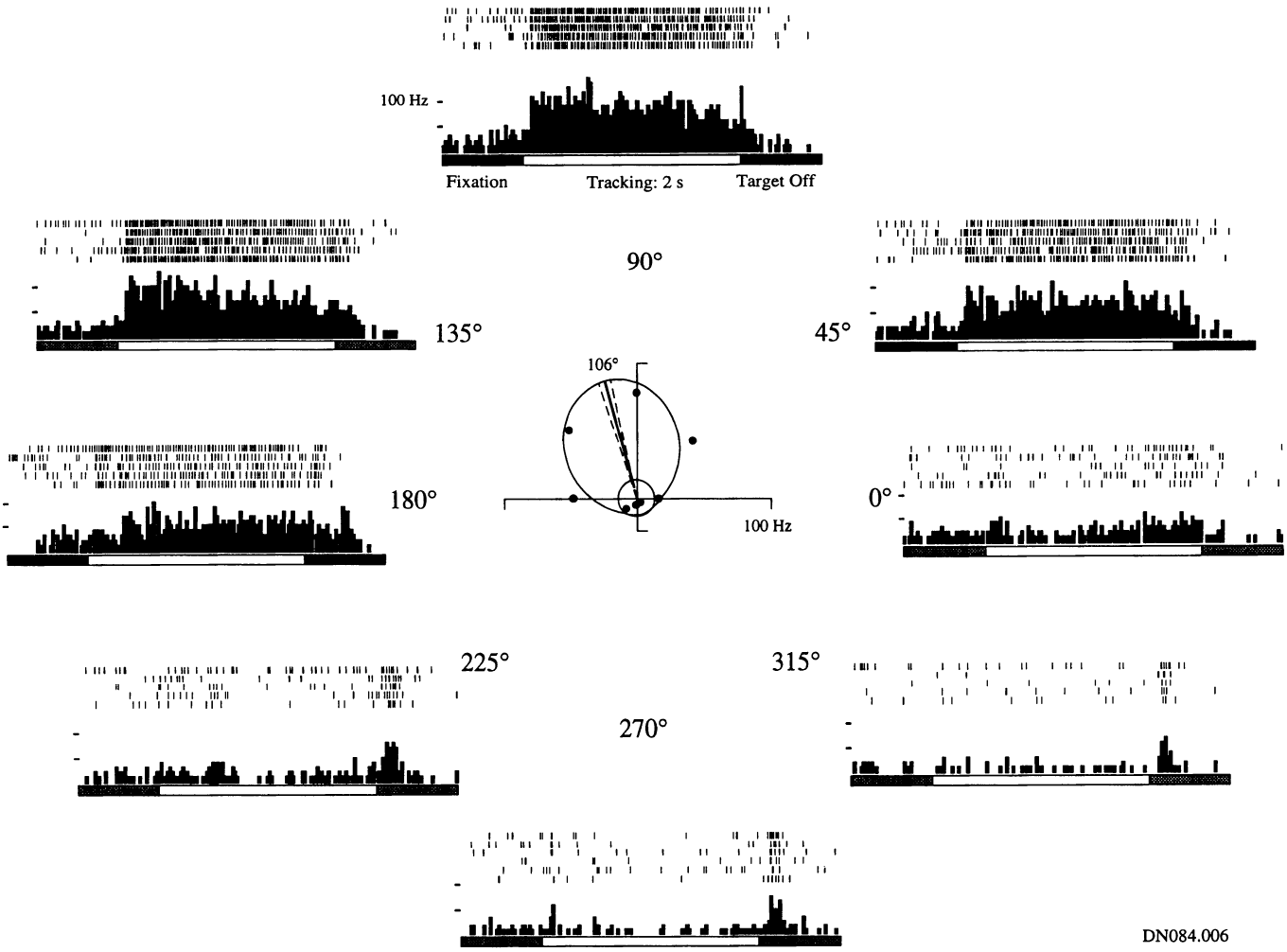

FIG. 3. Directional tuning of a pursuit neuron (*DN084*, right hemisphere). *Outer panels* show individual raster lines and response histograms averaged from 4–6 trials during constant-velocity tracking in 8 different directions. The target moved at 20°/s for 2 s with initial fixation at 20° eccentricity opposite impending tracking direction. Neuron responded tonically during upward and leftward tracking, between 45° and 180°, and did not respond or was inhibited during tracking in other directions. Note the transient inhibition following tracking in preferred directions (especially at 90° and 135°) and the excitation after tracking in nonpreferred directions (especially at 315° and 270°). *Center* is a polar plot of pursuit responses and their Gaussian tuning curve fit. Response rates (●) were averaged over the epoch of 100–2,000 ms after target motion began, across ≥5 trials in each direction. The tuning curve baseline (*inner circle*) was the average fixation rate in all trials, measured in the 250 ms preceding target motion onset. Tuning curve fit indicates a best direction of 106° (—) with a 95% confidence interval of (103°, 109°; - - -) and tuning index (σ) of 46°.

decreased with target velocity, however, this decrease reflected the interaction of a strong gaze preference of this neuron with how the velocity tests were arranged (to have 2 s of tracking, the faster trials were begun at more eccentric fixations, and this particular neuron was inhibited at the eccentric fixations away from its best tracking direction).

Quite similar sensitivity coefficients were obtained when the target velocity, as opposed to the monkey's average pursuit velocity, was used as the independent variable in the regression analysis. Sensitivities to target velocity ranged from 0.22 to 1.67, with an average of 0.77 spikes·s^{-1}·deg^{-1}·s^{-1}. Because target velocity and eye velocity were highly correlated in these tests, we cannot know to which velocity variable the neuronal responses are most closely related. Furthermore pursuit gain (the ratio of eye velocity to target velocity) usually decreased at higher pursuit/target velocities, implying a concomitant increase in retinal slip velocity. For example, in the data of Fig. 8, pursuit gain was high for the 2.5 and 5°/s conditions, but was smaller than 0.6 for the 25°/s condition, where eye velocity did not exceed 15°/s. Thus the target's increased retinal slip also could have contributed to the positive relationship between pursuit velocity and response rates.

Locations of pursuit neurons in relation to elicited SEM

Figure 10 shows the locations of pursuit neurons and of elicited SEMs in the three hemispheres that yielded the largest numbers of pursuit neurons. The smaller frontal cortex outlines show the entry points of all penetrations that encountered pursuit neurons, and the enlarged arcuate outlines summarize the recording and stimulation findings obtained in several penetrations (typically 2–10) at each of these locations. On the arcuate outlines, coordinates of pursuit neurons are marked by large black circles, those where smooth or saccadic eye movements, or both, were elicited electrically are marked by smaller circles (shaded, white, or

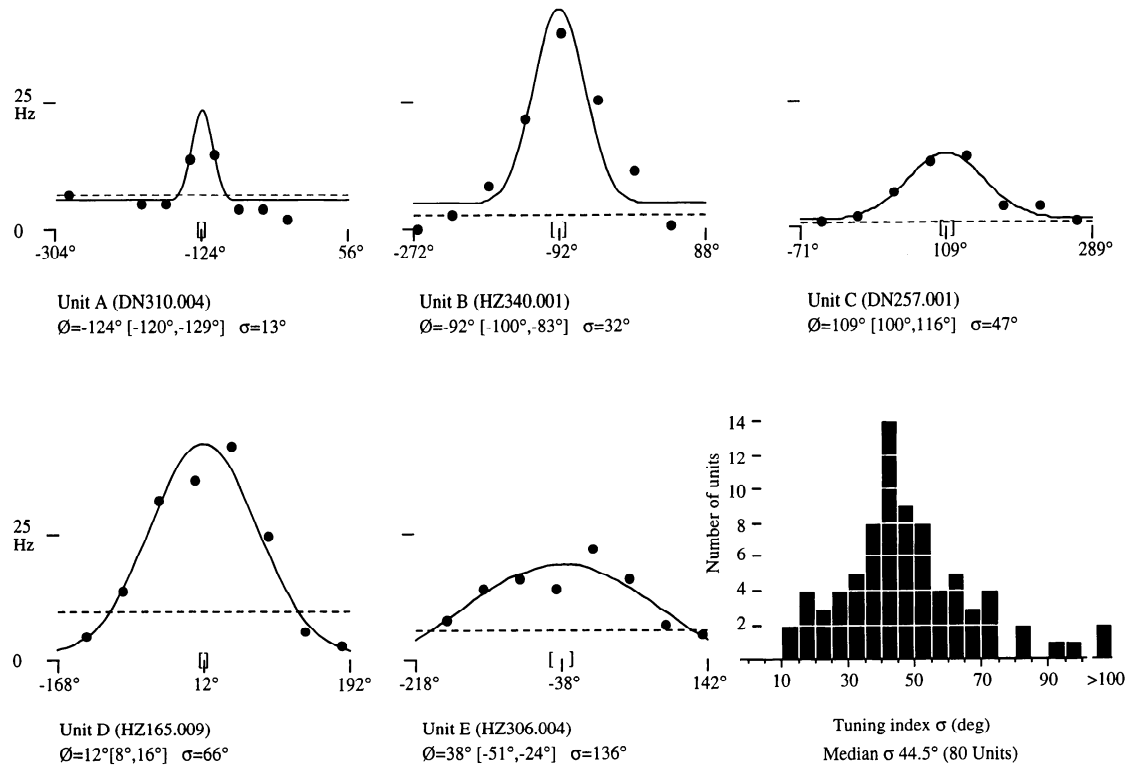

FIG. 4. Directional tuning of 5 pursuit neurons shown (*first 5 panels*). Directional tuning was tested with constant-velocity tracking, and response rates were averaged across the tracking period (2 or 0.75 s) as described in METHODS. Baseline rates (- - -) represent the average activity during fixation before target motion. Each tuning curve is centered on the neuron's best direction (ϕ; center tic on the abscissa), and other directions are indicated in a ($\phi - 180°$, $\phi + 180°$) convention. The 95% confidence intervals (*brackets on the abscissa*) also are indicated. These 5 examples were chosen to span the range of directional specificities seen and are arranged in order of increasing tuning index (σ). *Last panel* shows the distribution of tuning indices for all 80 pursuit neurons with quantitatively determined directional tuning.

shaded-and-white circles, respectively), and those where skeletal movements were elicited are marked by squares. Pursuit neurons were recorded in a circumscribed region in the arcuate fundus and posterior bank, lying approximately at the level of the principal sulcus. These neurons were found at virtually all coordinates that yielded elicited SEM and also at several locations adjacent to those of elicited SEM, where the microstimulation elicited saccadic eye movements, skeletal movements, or no movements. However, pursuit neurons were not encountered at coordinates clearly removed from the SEM region. Conversely, SEMs were never obtained from the vicinity of neurons with saccade-related responses.

Figure 11 shows two reconstructed electrode penetrations that coursed through the posterior arcuate bank and contained both pursuit neurons and elicited SEMs. Pursuit neurons were recorded at several sites and microstimulation at some of these sites evoked SEMs. As described below, the microstimulation elicited SEMs at only a small number of pursuit neuron sites, and the directions of these elicited SEMs generally matched the preferred directions of the pursuit neurons studied at their sites.

Correspondence between neurons' preferred pursuit direction and elicited SEM direction

In total, microstimulation was tested at 113 sites with pursuit neurons. Of these, SEMs were evoked at 27 sites, with some elicited saccades accompanying the SEMs at 13 of these sites. Purely saccadic eye movements (without SEMs) were evoked at 12 sites, and no eye movements were elicited from the remaining 74 sites using currents ≤ 100 μA.

To further investigate the relation between the recording and stimulation findings, we compared the directions of elicited SEMs with the preferred directions of pursuit neurons recorded at the stimulation sites. An example of such a comparison is shown in Fig. 12. The neuron recorded at this site had pursuit responses that were largest for tracking to the left and slightly down. A quantitative direction test involving eight different tracking directions yielded an estimated best direction of 212° with a tuning index (σ) of 45°. Microstimulation elicited SEMs that lasted throughout the stimulation train with eye velocities exceeding 20°/s at 50 μA. The elicited SEMs were directed down and to the left, regardless of the eye's orbital position at the time of stimulation, and the median direction of the elicited SEMs was 207°, very close to the neuron's preferred pursuit direction. For both these eye velocity traces and for the 2-D plots above, we used the stimulation and stabilization task; as we reported previously (Gottlieb et al. 1993), SEM velocities obtained in the stabilized condition usually exceed those obtained with stationary fixation targets.

As shown in Fig. 13, the preferred direction of most pursuit neurons predicted the direction of the SEMs subsequently elicited at their sites. Because these are both "circular" measures, the circular correlation coefficient r_+

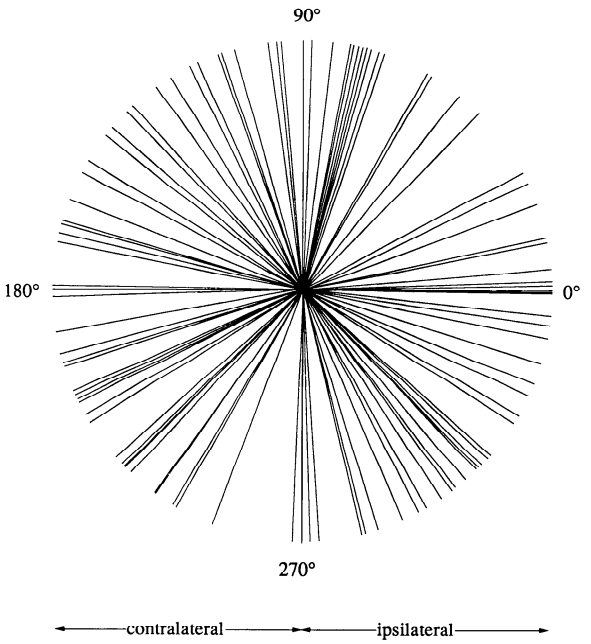

FIG. 5. Preferred tracking directions of 193 pursuit neurons. Preferred direction of each neuron, whether determined quantitatively ($n = 80$) or estimated with the interactive tasks ($n = 113$), is represented by the angle of one line. Directions of left hemisphere neurons are mirror-reversed to allow grouping of all data points as "contralateral" or "ipsilateral"; the horizontal component of the preferred tracking direction was ipsilateral in 93 neurons and contralateral in 97 neurons (the other 3 were judged vertical, 2 down and 1 up). Note that all tracking directions are represented fairly evenly with no apparent bias toward a major axis, nor toward contralateral or ipsilateral pursuit.

(Batschelet 1981, page 179) was used to measure their relationship. The resulting coefficient, 0.71, is highly significant ($P < 0.001$ for $n = 17$) by the Rayleigh test (Batschelet 1981, Table H). This agreement in direction, together with the agreement between the location of pursuit neurons and that of elicited SEMs, strongly suggests that microstimulation elicits SEMs by activating FEF pursuit neurons and, conversely, that FEF pursuit neurons are involved in pursuit generation under physiological conditions.

Despite the high overall correlation, however, at any given site the neuronal and elicited directions could differ substantially, with a mean discrepancy of 40° (median 42°; range 0–98°). This discrepancy may reflect errors in our estimation of neuronal preferred directions, caused in part by the broad directional tuning of pursuit neurons. In addition, the high current intensities often required to elicit SEMs (≤ 100 μA) may have activated remote pursuit neurons with somewhat different preferred directions from those of neurons near the electrode; however, stimulation current and directional discrepancy were not correlated in this sample.

As seen in Fig. 13, both the preferred pursuit direction of pursuit neurons where SEM was obtained, as well as the direction of the elicited SEM obtained at the sites of pursuit cells, were predominantly ipsilateral (11 of 17 in both cases fall between 90 and 270° in the Fig. 13 plot, in which the directions of sites in the right hemisphere are mirror reversed). This finding is not surprising, given that the SEMs elicited from the FEF are predominantly ipsilateral (Gottlieb et al. 1993). However, because FEF pursuit neurons appear to represent all directions fairly uniformly, this data suggests that pursuit neurons with ipsilateral preferences are involved more directly in pursuit generation than those with contralateral preferred directions.

In the saccadic part of FEF, saccades are elicited more readily (i.e., have lower thresholds) at the site of neurons with presaccadic responses relative to neurons with only postsaccadic responses (Bruce and Goldberg 1985). To determine whether an analogous effect might obtain in the SEM sector of FEF, we compared the response latencies relative to pursuit initiation of neurons at sites with elicited SEM to latencies at sites without elicited SEM. Pursuit units did tend to have longer leads at sites with elicited SEM, where their responses preceded pursuit onset by an average of 19.4 ms ($n = 23$; median 29.0 ± 72.4 ms mean ± SD), relative to those with no elicited movements, where unit responses preceded pursuit onset by an average of 15.7 ms ($n = 27$; median 19.0 ± 83.9 ms). However, these differences are not very large compared with the SD and were found not to be statistically significant by a Mann-Whitney U test. This lack of a robust effect may reflect some fundamental differences between processing in the saccadic and SEM parts of the FEF (see DISCUSSION).

DISCUSSION

Smooth-pursuit eye movements are thought to be controlled by cortico-ponto-cerebellar pathways, originating in primary visual cortex, involving extrastriate cortical areas specialized for visual motion processing, and effecting pursuit via a Purkinje cell discharge coding pursuit eye velocity (Lisberger et al. 1987). Figure 14 shows this basic pursuit circuit based on Leigh and Zee's findings (1991). Cells that discharge during smooth-pursuit tracking have been described in most parts of this circuit, including the medial superior temporal area (MST) (Komatsu and Wurtz 1988; Newsome et al. 1988; Thier and Erickson 1992), the posterior parietal lobule (Kawano 1984), the dorsolateral pontine nucleus (DLPN) (Mustari et al. 1988; Suzuki et al. 1990a; Thier et al. 1989), the dorsomedial pontine nucleus (DMPN) (Keller and Crandall 1983; Keller and Heinen 1991), and in floccular (Miles and Fuller 1975; Stone and Lisberger 1990ab) as well as the parafloccular (Noda and Mikami 1986) and vermal (Suzuki and Keller 1988ab) regions of cerebellar cortex.

In this report, we describe a class of neurons in the primate FEF that respond in relation to smooth pursuit but not to saccadic eye movements. These pursuit neurons were located in a circumscribed zone of the arcuate fundus and posterior bank, confirming and extending the earlier observation of several neurons deep in the arcuate sulcus that discharged in relation to smooth pursuit (Bruce et al. 1985). This report also complements our recent description of electrically elicited slow SEMs obtained by microstimulation in the arcuate sulcus (Gottlieb et al. 1993). Pursuit cells often were found at sites where SEMs were elicited, and the direction of elicited SEMs tended to match the preferred direction of pursuit neurons at that site. The properties of the pursuit neurons and their correspondence with SEMs support the hypothesis that these neurons con-

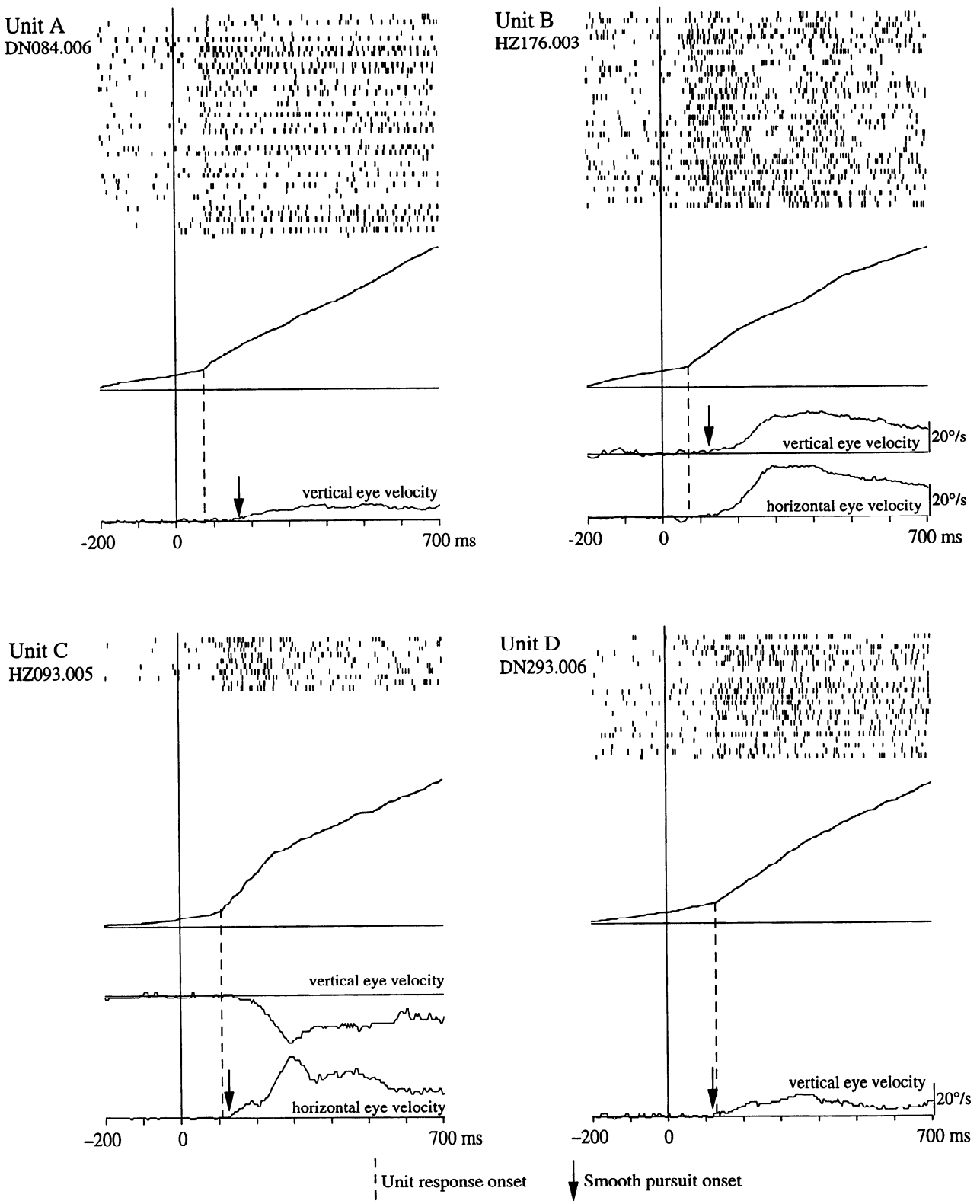

FIG. 6. Response latencies relative to smooth-pursuit initiation in 4 pursuit neurons. For each cell's experiment are shown, (*top to bottom*), individual raster lines, cumulative response histograms, and smooth-eye velocity traces averaged from 5–10 constant-velocity tracking records after removing saccades (only the initial 750 ms of tracking are shown regardless of total track duration). Neural response latencies (- - -) shown as read from the inflection points in the cumulative histograms; arrows indicate estimated beginning of pursuit. Neurons are arranged in order of decreasing lead time of their response relative to pursuit initiation. *Neurons A–C* began responding, respectively, at 71, 70, and 104 ms after target motion began, and led pursuit initiation by 90, 48, and 21 ms. *Neuron D* began responding 125 ms after target motion and lagged pursuit initiation by 10 ms. Eye records represent tracking along the neuron's best directions (90, 45, 315, and 90° in *neurons A–D*, respectively). Raster lines and cumulative histograms were taken during tracking in 8 different directions for *neurons A* and *B*, during tracking at 315° for *neuron C*, and during upward tracking at different speeds (2.5–25°/s) for *neuron D*. This arrangement departs from our usual analysis, where we considered only neural activity associated with a neuron's preferred direction or speed.

tribute to the generation of pursuit and, conversely, that microstimulation in this part of FEF evokes SEMs by activating such neurons and hence their connections to other parts of the pursuit system. Thus these data help provide a physiological substrate for the pursuit deficits obtained with experimental lesions involving the arcuate fundus (Keating 1991, 1993; Lynch 1987; MacAvoy et al. 1991), and agree with existing anatomic evidence connecting FEF into the pursuit circuitry of Fig. 14, as discussed further later.

Nature and specificity of pursuit responses in FEF

FEF pursuit neurons responded during smooth-pursuit tracking of visual stimuli moving in a particular, preferred direction. Responses typically began shortly after the start of target motion usually just before the eye actually started to move, as discussed further later. When tracking constant-velocity target motion, some neurons responded tonically throughout the entire track across the screen, some responded only or primarily at the start of the track, and some were intermediate in that their response diminished after a few hundred milliseconds but did not completely stop until after the target was extinguished at the end of the trial. During the tracking of sinusoidal target motion, most cells responded in a very phase-locked fashion.

We are certain that these cells have bona-fide smooth-pursuit responses that are not based on other previously reported responses of FEF cells. First, we were careful to rule out saccade-related responses inasmuch as Bruce and Goldberg (1985) reported that 50% of cells in the main part of FEF, where saccades can be elicited electrically, had presaccadic responses, visual or motor or both, and that many of the remaining cells responded postsaccadically (see also Bruce et al. 1985; Goldberg and Bruce 1990; Schall 1991). Unlike the saccade-related cells, pursuit cells did not respond when tested on standard visually guided saccade tasks. Furthermore, their pursuit responses were not correlated with catch-up saccades made during pursuit. Thus saccadic and pursuit responses seem to be found on exclusive sets of FEF cells, largely in different sectors. This finding also indicates that electrical elicitation of combined saccades and SEM seen at some sites probably reflects current spreading into both sectors.

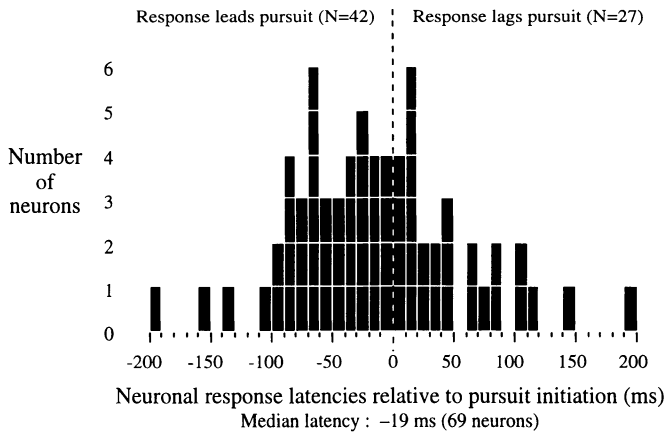

FIG. 7. Response latencies relative to pursuit onset for 69 pursuit neurons. These latencies were calculated by subtracting neural response latencies from pursuit-eye movement latencies, both measured relative to the start of target motion. Thus negative ($n = 42$) and positive ($n = 27$) values represent, respectively, lead and lag times of neuron responses relative to pursuit initiation.

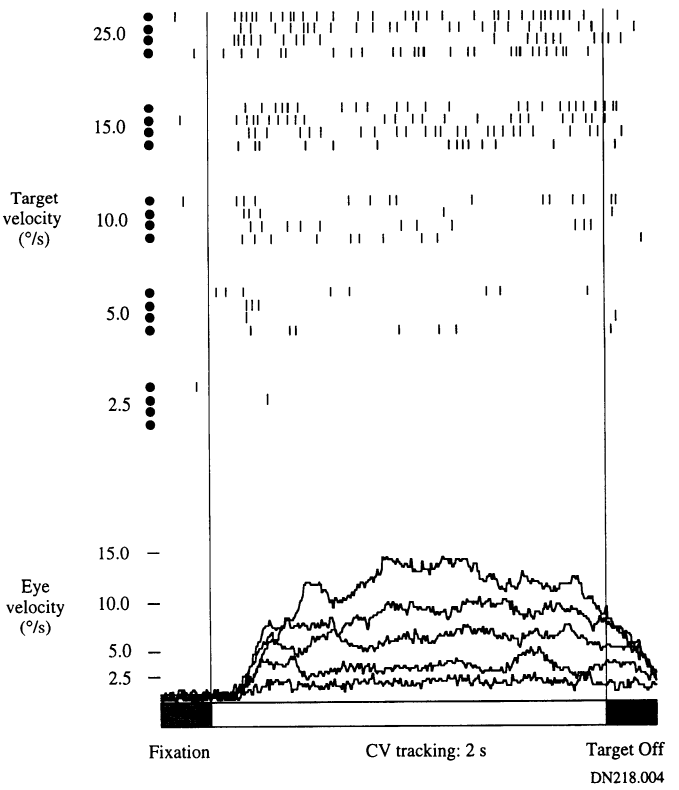

FIG. 8. Velocity sensitivity of a pursuit neuron (*DN218*, left hemisphere). Tracking targets moving at constant velocities of 2.5, 5, 10, 15, and 25°/s, all at polar direction 45° (close to the neuron's preferred direction) were presented in random order. Individual response rasters shown (*top*) grouped according to target velocity. Four trials (●) were conducted for each velocity. Neuron did not respond during the last 2 trials in the 2.5°/s condition. Superimposed eye velocity traces (*bottom*), that were averaged from 4 trials taken at 1 target speed after removing the saccades. Note that, because pursuit gain fell with increasing target velocity (being slightly <0.6 for the 25°/s condition), the average retinal slip also increased in parallel with target and eye velocities.

Similarly, the FEF pursuit neurons are distinct from the orbitally sensitive FEF units first described by Bizzi (1968), and later by Bizzi and Schiller (1970), Bruce and Goldberg (1985), and Schall (1991). Bizzi (1968) noted that such units seemed to have a pursuit response; however, they responded only when the pursuit movement carried the eye into their preferred orbital location. In contrast, all of our pursuit cells were selective for pursuit direction and did not respond, or were suppressed below baseline, when the same orbital space was retraversed by pursuing opposite to their preferred direction. The discharge of some pursuit neurons was modulated significantly by the eye's orbital position; however, these cells remained tuned for pursuit direction regardless of the orbital location of the pursuit.

Likewise, FEF pursuit responses do not appear to be entirely controlled by any single component of the general pursuit situation, such as visual activation of a discrete, motion-sensitive receptive field by the retinal slip of the pursuit target, or an activation by an efferent copy of eye velocity signals in the brain stem. Most FEF pursuit cells had at least

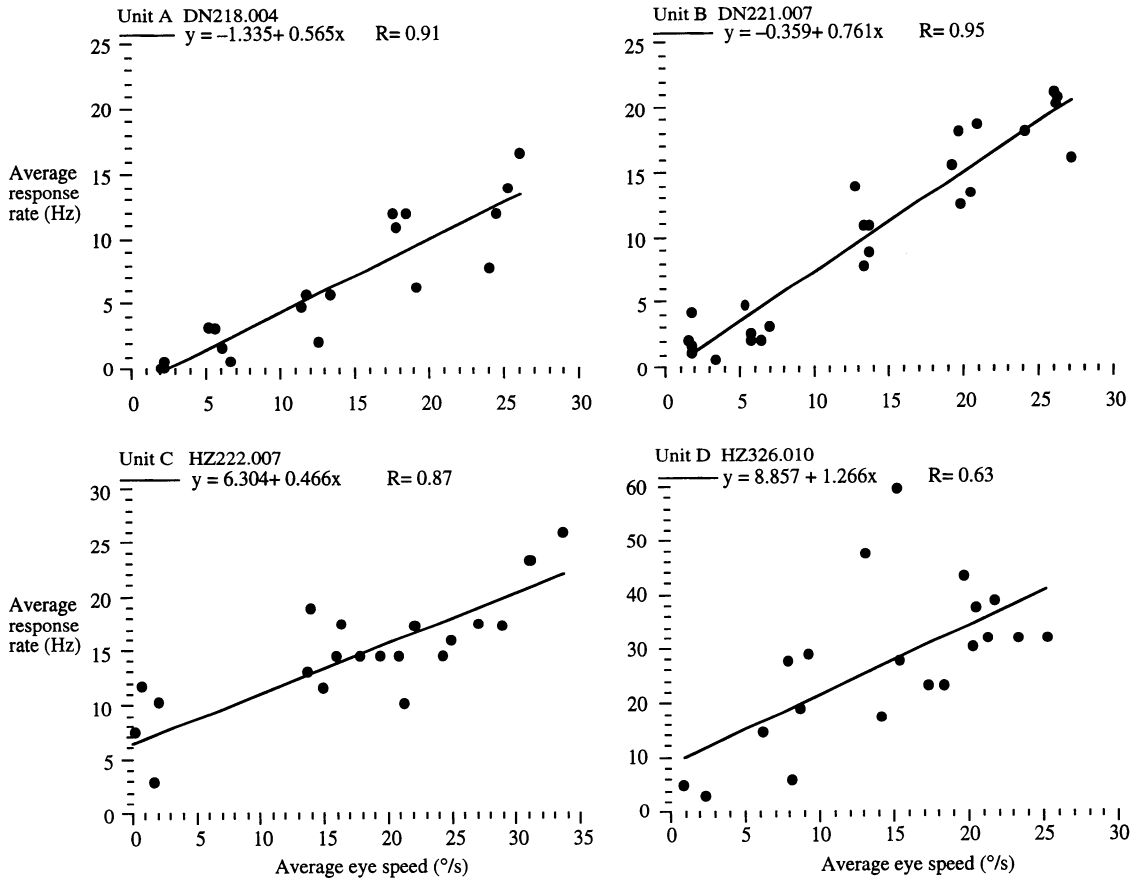

FIG. 9. Velocity sensitivities of 4 neurons with pursuit responses, with *neuron A* the same as that in the previous figure. Each neuron was tested during constant-velocity tracking directed along its preferred direction, at velocities ranging from 2.5 to 50°/s. Response rates and eye velocity were averaged across the entire 2 s of tracking for each trial. Regression equation ($y = a + bx$) and the correlation (R) are given above each plot. All the correlations and multiplication coefficients (b) are significant at the 0.05 level.

some responses to peripheral visual motion in their preferred pursuit direction during continued stationary fixation; however, when identical retinal motion was used to initiate smooth pursuit, then the responses were stronger and more sustained. In having such passive visual-motion responses, FEF pursuit cells are similar to cells throughout the pursuit circuit of Fig. 14, even in structures clearly downstream from FEF. For instance, most pursuit cells in DLPN have such visual-motion responses (Mustari et al. 1988; Suzuki et al. 1990a; Thier et al. 1988), and even the floccular Purkinje cells that discharge in proportion to ipsilateral pursuit velocity (Miles and Fuller 1975) are now known to have a phasic response to visual motion (Krauzlis and Lisberger 1991; Stone and Lisberger 1990a,b). Conversely, the pursuit responses could not be understood as simply deriving from an efferent copy of smooth eye velocity projected along the cell's preferred pursuit direction. Not only did the responses usually precede the start of the smooth movement, but they usually diminished as eye velocity approached target velocity. Furthermore as just discussed, most pursuit cells still responded to peripheral visual motion during continued fixation at 0 eye velocity. We defer a detailed analysis of the sensitivity of FEF pursuit cells to visual motion (i.e., retinal slip), and of their sensitivity to extraretinal factors such as orbital position and eye velocity, for a separate report in preparation.

Coding of pursuit direction

All pursuit neurons were tuned directionally, that is, their responses were strongest during pursuit in one (preferred) direction, and declined progressively with pursuit at larger angles from that direction. Fitting the responses during pursuit in different directions to a Gaussian function revealed that these neurons had a wide range of tuning widths, with a median tuning index of 44.5°, corresponding to an average full width at half maximum of 105°.

The broad overall directional tuning implies that most FEF pursuit neurons respond during pursuit in many different directions (e.g., most still gave >50% of their maximal rates during tracking removed by 45° from their optimal directions) and, consequently, that a large number of FEF pursuit neurons are likely to be active during pursuit in a single given direction. The direction of a pursuit eye movement thus may be coded by a weighted vector average of the optimal directions of all the neurons active at that time, as has been suggested for coding of reaching movement directions in the motor cortex (see Georgopoulos 1986). Under this hypothesis, pursuit direction would be closest to the optimal direction of the pursuit neurons responding most strongly at a given time, or, during microstimulation, to the optimal directions of the neurons nearest the electrode. Consistent with this prediction, each SEM site has a charac-

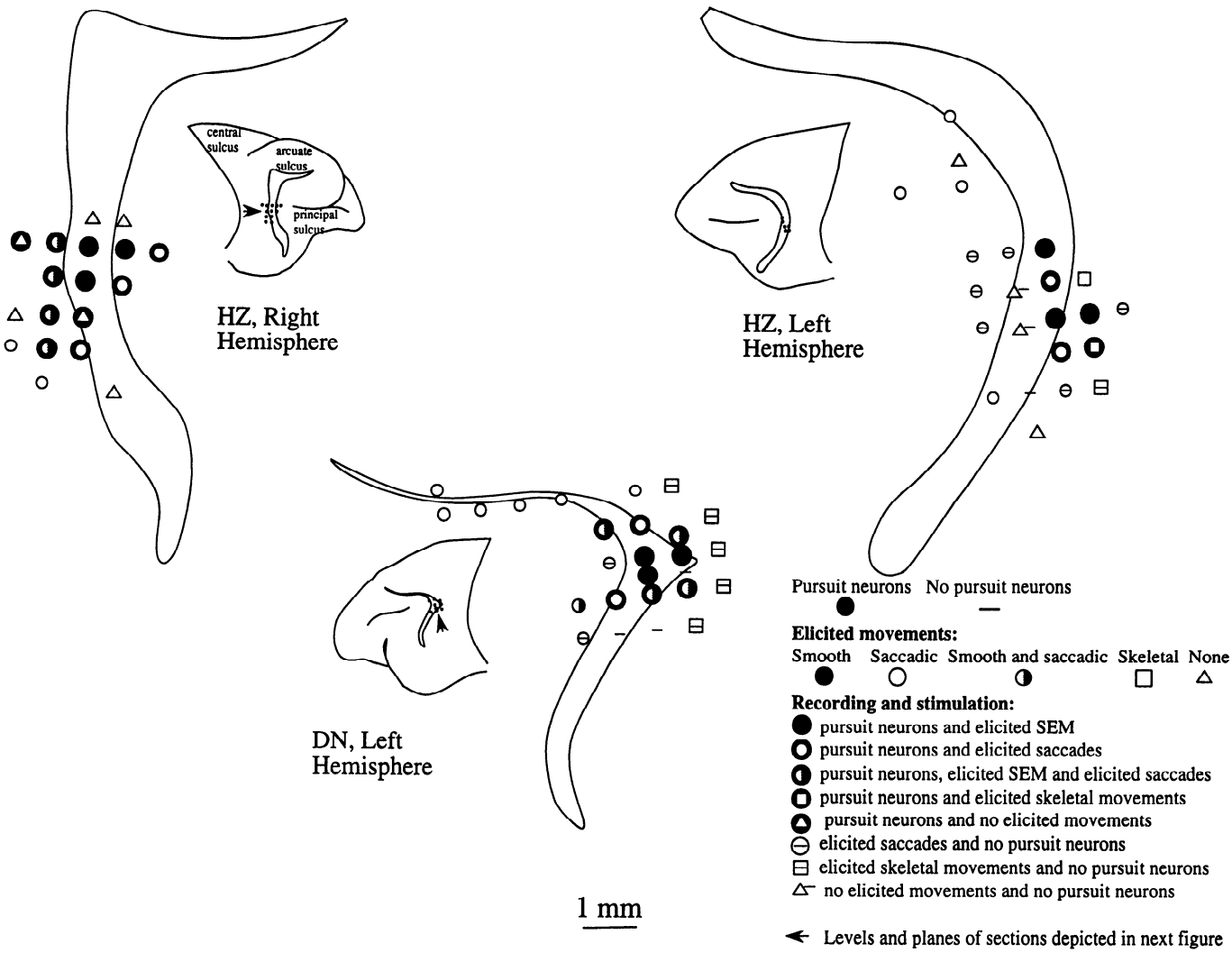

FIG. 10. The entry points and physiological findings of all penetrations in the FEF region of 3 hemispheres. Maps are reconstructed with reference to the entry points of penetrations directly identified on the basis of iron deposits or marking lesions. Locations relative to frontal lobe landmarks of penetrations in which pursuit neurons were encountered are depicted (*insets*). Enlarged outlines of the arcuate sulci show in more detail the physiological findings at each surface coordinate explored, typically summarized from 2 to 10 penetrations. Level and planes of the sections shown in the next figure (→ on frontal lobe outlines). Neurons with pursuit responses (●) were recorded in circumscribed regions of both arcuate banks, approximately posterior to the principal sulcus. Within this region, eye movements (smooth, saccadic, or both smooth and saccadic) were often elicited. Pursuit neurons were recorded at all coordinates from which smooth eye movements (SEMs) were elicited electrically, however, SEMs were not elicited from a number of locations with pursuit-responsive neurons. At these coordinates, we elicited saccadic movements, skeletal movements (at one location in the left hemisphere of *monkey HZ*), or did not elicit eye movements. Right hemisphere of *monkey HZ* was distorted by a brain edema that developed during recording.

teristic SEM direction that is relatively independent of stimulation current (Gottlieb et al. 1993).

The significant correlation between elicited SEM directions and the optimal directions of pursuit neurons at the stimulation sites strongly supports the hypothesis that stimulation in this part of FEF elicits SEMs by activating pursuit neurons and hence their connections to the pursuit system. The relatively large discrepancy, ~40° on average, between elicited SEM direction and the optimal directions of neurons at the stimulation sites was probably due to the large currents (50–100 μA) typically required to elicit SEMs. These current intensities were likely to activate more distant neurons and fibers whose directions varied from the neurons we actually recorded. These currents were about twice those used in the saccadic FEF, where the differences between the directions of elicited saccades and the optimal directions of neurons at the stimulation sites were smaller than those we report (Bruce et al. 1985, Fig. 4). Errors of estimation of neuronal best directions caused by the broad directional tuning of pursuit neurons also may have contributed to this discrepancy.

The finding that FEF pursuit neurons represent all possible pursuit directions, whereas FEF microstimulation elicits predominantly ipsilateral SEMs (Gottlieb et al. 1993) suggests that ipsilaterally tuned FEF pursuit neurons are relatively more directly involved in pursuit generation than the contralaterally tuned units. The latter neurons may serve instead to inform the ipsilateral FEF of ongoing contralateral pursuit or visual motion or may be relatively weakly connected to the pursuit system. This hypothesis is

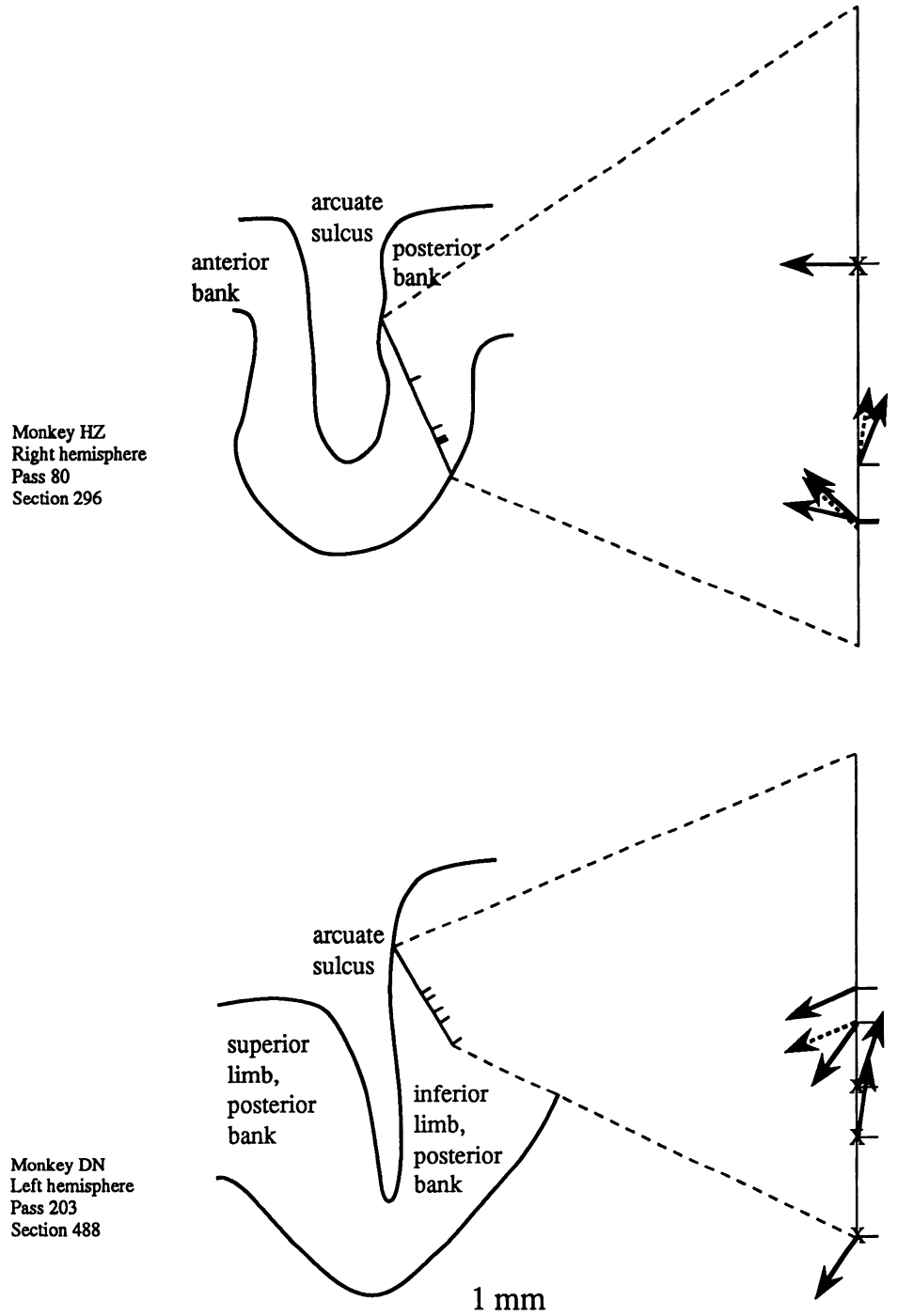

FIG. 11. Examples of individual penetrations where pursuit neurons and elicited SEMs were obtained. Planes and locations of the sections outlined here are indicated (→) in the corresponding hemispheres of Fig. 10. Note that the brain of *monkey HZ* was sectioned in a plane approximately perpendicular to the arcuate sulcus at its most posterior extent, whereas the coronal plane was used in *monkey DN*. Locations of these penetrations (both in the posterior bank of the arcuate sulcus) were reconstructed on the basis of iron deposits made in subsequent penetrations at the same coordinates. Depths of pursuit neurons (—) were obtained by comparing the depth of each recording site with entrance and exit from gray matter as well as with the depth of the iron deposits. Top penetration ended when the electrode exited gray matter and no more neurons were recorded, whereas the bottom track was discontinued while the electrode was still in gray matter. Expanded drawings of the tracks (*right*) show the neurons' preferred tracking directions (→) and the elicited SEM directions (- - →). Note that the preferred directions of these neurons could be contralateral or ipsilateral relative to their hemisphere and that SEMs were elicited from a subset of sites with pursuit neurons, whereas at other sites no eye movements were elicited (X). When obtained, elicited SEMs were usually directed along the preferred tracking directions of neurons at the stimulation site.

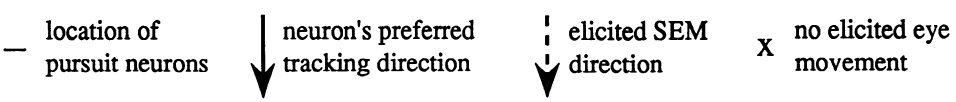

consistent with the finding that unilateral FEF lesions compromise primarily ipsilateral pursuit (MacAvoy et al. 1991).

Similar to the findings in FEF, lesions and microstimulation in MST and the foveal representation of area MT primarily affect ipsilateral pursuit (Dursteler and Wurtz 1988; Komatsu and Wurtz 1989), but the pursuit neuron populations in these areas show little or no bias for ipsilateral directions (Komatsu and Wurtz 1988). Similar results are obtained in the DLPN (May et al. 1985, 1988; Mustari et al. 1988). A clear bias in neural responses first appears in the cerebellum, with ipsilateral pursuit preferred by 80% of the

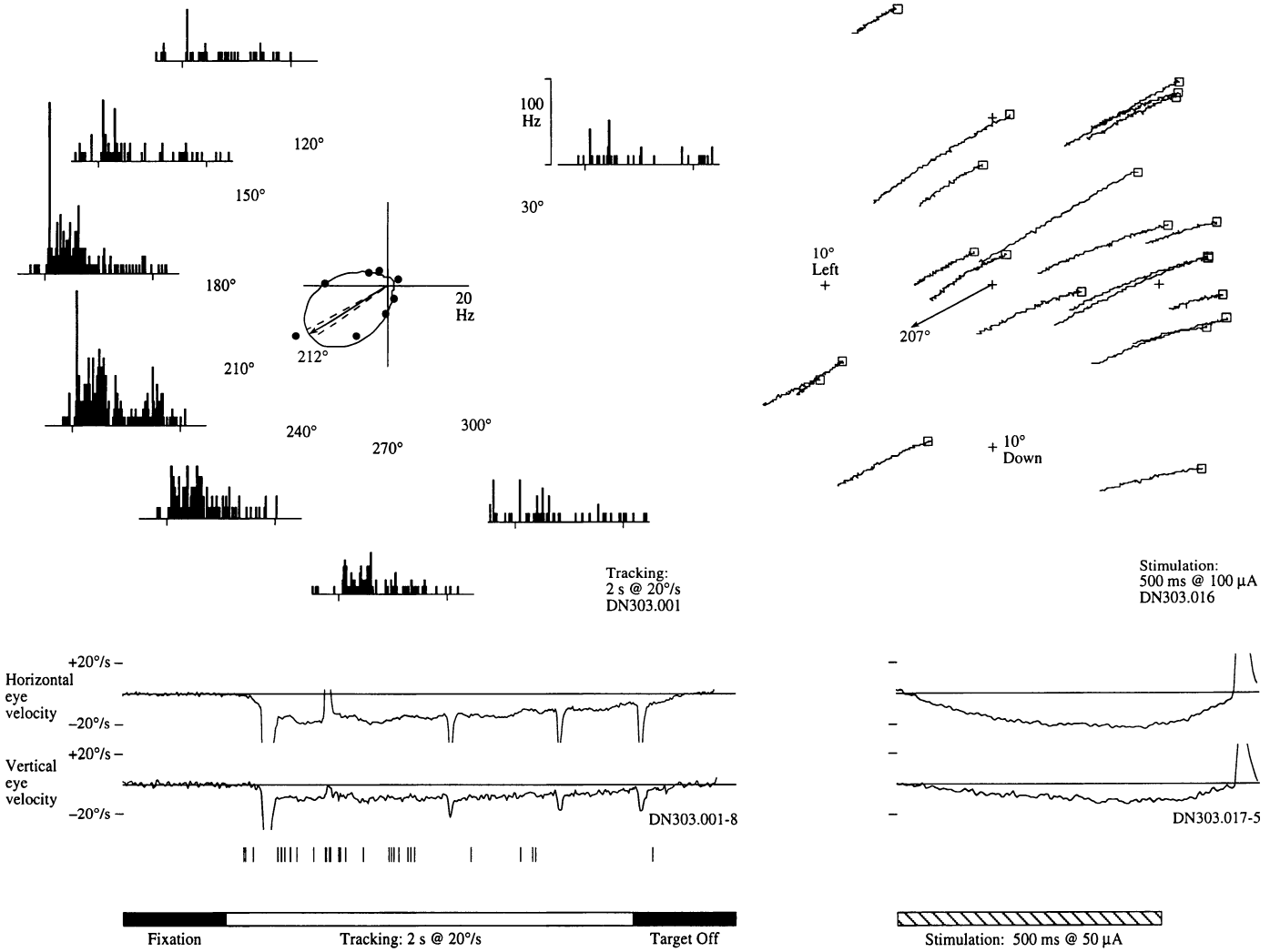

FIG. 12. Responses of a pursuit neuron (*DN303*, left hemisphere) and the SEMs electrically elicited at the site of that neuron. Responses (*top left*) during constant-velocity tracking at 20°/s in 8 different directions. Beginning of target motion is indicated by the first tic on the abscissa in each histogram and target disappearance at the end of the track by the second tic. Polar response plot (*center*) was constructed using response rates averaged over the entire tracking interval for each of the 8 directions. Gaussian fit of these responses indicates a best direction of 212° and a tuning index (σ) of 45°. Eye velocity traces and spikes (*bottom left*) for a single tracking trial along a preferred direction (210°). Two-dimensional plots (*top right*) of SEM elicited from various initial fixation positions (□). Note that the SEMs were directed down and to the left regardless of the eye's orbital position, with a median direction of 207° (→). Horizontal and vertical eye velocity traces (*bottom right*) of SEM elicited with electrical stimulation during fixation of a foveally stabilized fixation target. Other aspects of this particular cell's responses were shown in Fig. 2.

floccular Purkinje cells (Lisberger and Fuchs 1978; Stone and Lisberger 1990a,b) and 60% of the vermal pursuit cells (Suzuki and Keller 1988a,b). It would be interesting to know if the ipsilaterally tuned FEF cells provide most of the corticopontine fibers from the pursuit part of FEF. The ultimate laterality of the multisynaptic pathway from pursuit-FEF through the pons to cerebellar cortex also needs to be determined.

Coding of pursuit velocity

Many FEF pursuit neurons were sensitive to tracking velocity, their responses increasing with target velocities in the range tested (2.5–50°/s). The lack of an "optimal" velocity for pursuit neurons (at least in the optimal velocity range for smooth pursuit eye movements) (see Lisberger et al. 1987) suggests that pursuit magnitude is coded by the intensity of neural activity ("rate code") and not by the location of neural activity ("place code"). This rate code hypothesis is consistent with our previous finding that elicited SEM velocities and accelerations are increasing functions of the stimulation current intensity and thus are not constant at a given site (Gottlieb et al. 1993). However, it is unclear whether the neurons' increasing response rates with increasing target speed reflected the higher pursuit velocities or the higher eye accelerations elicited by faster targets. In addition, because the monkeys' pursuit gain (the ratio of eye velocity to target velocity) generally decreased with higher target velocities, thereby producing larger retinal slips, these increasing responses may have reflected a sensitivity to retinal slip magnitude.

The velocity sensitivity (the linear regression slope) of

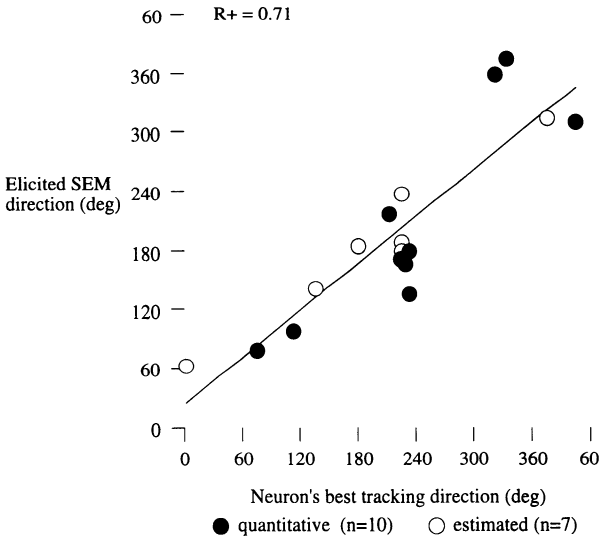

FIG. 13. Relationship between the preferred tracking direction of pursuit neurons and the direction of electrically elicited SEMs. For each of 17 sites, the median direction of the elicited SEM is plotted against the preferred tracking direction of a neuron recorded at that site. Directions of right hemisphere sites were mirror reversed so that ipsilateral directions fall between 90° and 270° for both right and left hemisphere sites. Preferred tracking direction either was estimated using the interactive versions of the constant velocity or sinusoidal tracking tasks (7 sites, ○) or was determined from Gaussian fit of quantitative data (10 sites, ●). As explained in the text, the circular correlation coefficient r_+ (Batschelet 1981, p. 179) was used to measure their relationship. Resulting coefficient, 0.71, is highly significant ($P < 0.001$ for $n = 17$). In contrast, the conventional correlation of the direction pairs as plotted ($r = 0.89$) exaggerates their agreement because for some directions an equivalent value >360 was used to emphasize their relation in the plot.

FEF pursuit neurons, 0.24–1.42 spikes·s^{-1}·deg^{-1}·s^{-1}, was similar to the sensitivities of floccular gaze velocity Purkinje cells (0.90–1.02 spikes·s^{-1}·deg^{-1}·s^{-1}) (Lisberger and Fuchs 1978; Stone and Lisberger 1990a) and of DLPN eye movement neurons (0.2–2.0 spikes·s^{-1}·deg^{-1}·s^{-1}) (Mustari et al. 1988). FEF neurons responded better to higher tracking velocities than posterior parietal pursuit units, which are maximally sensitive to tracking velocities up to 10°/s and saturate thereafter (Kawano et al. 1984).

The use of a rate code to represent tracking velocity in the pursuit part of FEF contrasts with the saccadic part of FEF, where both saccade directions and amplitudes are represented in place codes (Bruce and Goldberg 1985; Robinson and Fuchs 1969). This difference may reflect a closer participation of pursuit-FEF neurons in the ongoing control of smooth-eye movements. Saccadic-FEF neurons can trigger saccades but are not thought to control directly the duration or velocity profile of the saccade via the duration or intensity of their burst (Segraves and Park 1993). Instead, saccade amplitude is represented in a topographic manner across the saccadic FEF: small saccades are represented ventrally and deep in the sulcus whereas large saccades are represented dorsally and near the sulcal lip (see Bruce et al. 1985). This difference in the coding of the eye movement's magnitude dimension (smooth-velocity/saccade-amplitude) may help explain how the pursuit FEF can be so much smaller than saccadic FEF, the explanation being that pursuit FEF only represents one parameter (pursuit direction) with a place code whereas saccadic FEF appears to represent all combinations of two parameters (saccade direction and size) with a place code.

Coding of pursuit initiation

Most FEF pursuit neurons began responding before the onset of the pursuit eye movements indicating that they could participate in pursuit initiation. This possibility is supported by the finding that stimulation in this part of FEF elicits SEMs from stationary fixation and that increases in stimulation current increase smooth-eye acceleration (Gottlieb et al. 1993).

The finding that lead times of neuronal responses relative to pursuit onset tended to be longer at sites with elicited SEMs than at those with no elicited eye movements lends

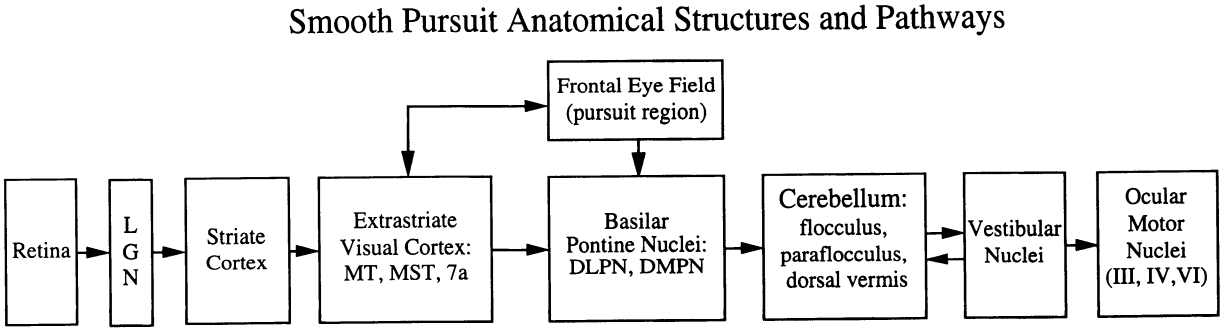

FIG. 14. Cortico-ponto-cerebellar circuitry thought to underlie the smooth pursuit system in the primate. Diagram follows Fig. 4.6 of Leigh and Zee (1991). FEF connectivity, including the feedback to the extrastriate box, is based on known connections of the saccadic part of FEF and of the general FEF region without physiological specification; further delineation of specific cortico-cortical and cortico-pontine pathways involving FEF awaits tracer injections into the smooth pursuit part of FEF. LGN, lateral geniculate nucleus; MT, middle temporal area; MST, medial superior temporal area; DLPN, dorsolateral pontine nucleus; DMPN, dorsomedial pontine nuclei. Additional structures could be included at most levels. At the cortical level, motion sensitive neurons in the fundal superior temporal area (FST), the ventral intraparietal area (VIP), and the superior temporal polysensory area (STP) could participate in pursuit. At the pontine level, the nucleus reticularis tegmenti pontis (NRTP) and the lateral pontine nuclei (LPN) also may carry pursuit signals. At the vestibular nucleus level, the nucleus prepositus hypoglossi (NPH) also may help carry smooth-eye velocity; interestingly, FEF may have a direct projection to NPH (Leichnetz 1985; Stanton et al. 1988). See also Keller and Heinen (1991, Fig. 9), Tusa and Ungerleider (1988, Fig. 7), Lisberger et al. (1987, Fig. 5), Fuchs and Mustari (1993), Boussaud et al. (1990), and Leichnetz (1989) for further anatomic details.

further support to the above hypothesis. This result seems analogous to the finding that, in the saccadic FEF, the lowest thresholds for evoking saccades are obtained at sites of presaccadic neurons (those responding before the saccade), whereas higher thresholds characterize sites of purely postsaccadic neurons (those responding only after saccades) (Bruce et al. 1985). The failure of this latency difference to reach significance in the pursuit FEF may be explained in part by the wide variations in response latencies among pursuit neurons. Alternatively, it may reflect the fact that, whereas FEF presaccadic neurons are believed to act primarily as triggers for stereotyped saccades, pursuit neurons are likely to participate in the on-line guidance of pursuit. Thus neurons that begin firing after pursuit onset still may contribute to late stages of pursuit initiation and to pursuit maintenance. Interestingly, some DLPN units also begin firing only after pursuit onset (Mustari et al. 1988).

The present experiments do not establish whether the early, prepursuit responses of FEF neurons were primarily visual (in other words, conditional upon the pursuit target beginning its movement in the neuron's receptive field) or primarily related to the initial smooth-eye acceleration. It is clear that most pursuit cells have at least a weak response to visual motion in the absence of pursuit; however, because pursuit onset is almost always visually driven and initial smooth-eye accelerations correlate with the retinal slip velocity immediately preceding pursuit onset (Lisberger et al. 1987), if these responses correlated with the retinal slip during the pursuit latency period, they are also likely to correlate with the initial smooth-eye accelerations.

FEF's place within the smooth-pursuit system

As mentioned earlier, smooth-pursuit eye movements appear to be controlled by a cortico-ponto-cerebellar pathway. Although the anatomic connections specific to the pursuit part of FEF have not yet been described, the larger FEF region is connected with important parts of this smooth pursuit circuit. First, FEF is reciprocally connected with the middle temporal and middle superior temporal areas MT and MST (Boussaud et al. 1990; Huerta et al. 1987; Leichnetz 1989; Stanton et al. 1994; Ungerleider and Desimone 1986) that appear to provide the visual motion information used for pursuit (Dursteler and Wurtz 1988; Komatsu and Wurtz 1989; Newsome et al. 1985). The FEF is also connected with the parietal lobe area VIP and temporal lobe areas FST and STP. Like MT and MST, these cortical areas also have many cells sensitive to visual motion, although it is less clear that they are involved in smooth pursuit. The MT and MST areas appear to provide the visual motion information used for pursuit (Dursteler and Wurtz 1988; Komatsu and Wurtz 1989; Newsome et al. 1985).

Like MT and MST, FEF projects to basilar pontine nuclei, including the dorsolateral and dorsomedial pontine nuclei (DLPN and DMPN) (Huerta et al. 1986; Leichnetz 1989; Stanton et al. 1988). Based on this connectivity, we located the pursuit-FEF box in Fig. 14 such that it is downstream of the extrastriate motion areas and yet projects to the pons in parallel with them.

In several ways, the situation of FEF in the Fig. 14 circuit is supported by functional, as well as anatomic, considerations. First of all, its placement in a parallel pathway agrees with the effects of experimentally removing FEF. In monkeys, FEF lesions involving the arcuate fundus where the pursuit FEF is located cause profound tracking deficits (Keating 1993; Lynch 1987; MacAvoy et al. 1991); however, this deficit involves a substantial reduction in pursuit gain, but not a complete loss of pursuit. Moreover, there can be considerable, though not complete, recovery of pursuit gain over several months following the lesion (Lynch 1989; MacAvoy et al. 1991). FEF lesions in humans also reduce smooth pursuit gain without eliminating pursuit (Pierrot-Deseilligny 1994). Similarly, the eye-tracking impairment associated with schizophrenia (Holzman 1987; Levy et al. 1993), and which may reflect a frontal lobe dysfunction (Levin 1984; Weinberger et al. 1986), is primarily characterized by a diminished smooth-pursuit gain (e.g., Abel et al. 1991).

Our physiological data so far suggests that FEF provides an acceleration-type signal related to pursuit initiation and maintenance. However, it is not clear how, in the context of the closed-loop pursuit system, an acceleration deficiency would significantly diminish asymptotic pursuit velocity. Grasse and Lisberger (1992) recently hypothesized that the FEF is separate from the signals used to drive pursuit, but can potentiate high pursuit gains by closing a "switch", which completes the pursuit circuit. Thus the FEF pursuit responses would represent a pursuit decision, rather than a signal directly controlling or reflecting pursuit magnitude. Further research will be necessary to see if this is the mechanism by which FEF cortex helps govern pursuit gain.

We thank G. Leydon for providing computer programs used for data analysis and illustration and P. S. Goldman-Rakic, J. Hirsch, and R. H. LaMotte for critical comments on earlier drafts of the manuscript.

This work was supported by National Eye Institute Grant EY-04740 and National Institute of Mental Health Grant MH-44866.

Present address and address for reprint requests: J. P. Gottlieb, Uniformed Services University of Health Sciences, Department of Anatomy, 4301 Jones Bridge Road, Bethesda MD 20814.

Received 8 February 1993; accepted in final form 25 May 1994.

REFERENCES

ABEL, L. A., FRIEDMAN, L., JESBERGER, J., MALKI, A., AND MELTZER, H. Y. Quantitative assessment of smooth pursuit gain and catch-up saccades in schizophrenia and affective disorders. *Biol. Psychiat.* 29: 1063–1072, 1991.

BATSCHELET, E. *Circular Statistics in Biology.* London: Academic, 1981.

BIZZI, E. Discharge of frontal eye field neurons during saccadic and following eye movements in unanesthetized monkeys. *Exp. Brain Res.* 6: 69–80, 1968.

BIZZI, E. AND SCHILLER, P. H. Single unit activity in the frontal eye fields of unanesthetized monkeys during eye and head movement. *Exp. Brain Res.* 10: 150–158, 1970.

BOUSSAOUD, D., UNGERLEIDER, L. G., AND DESIMONE, R. Pathways for motion analysis: cortical connections of the medial superior temporal and fundus of the superior temporal visual areas in the macaque. *J. Comp. Neurol.* 296: 462–495, 1990.

BRUCE, C. J. Integration of sensory and motor signals for saccadic eye movements in the primate frontal eye fields. In: *Signal and Sense, Local and Global Order in Perceptual Maps,* edited by G. M. Edelman, W. E. Gall, and W. M. Cowan. New York: Wile-Liss, 1990, p. 261–314.

BRUCE, C. J. AND GOLDBERG, M. E. Primate frontal eye fields. I. Single neurons discharging before saccades. *J. Neurophysiol.* 53: 603–635, 1985.

BRUCE, C. J., GOLDBERG, M. E., BUSHNELL, M. C., AND STANTON, G. B.

Primate frontal eye fields. II. Physiological and anatomical correlates of electrically evoked eye movements. *J. Neurophysiol.* 54: 714–734, 1985.

CRIST, C. F., YAMASAKI, D. S. G., KOMATSU, H., AND WURTZ, R. H. A grid system and a microsyringe for single cell recording. *J. Neurosci. Methods* 26: 117–122, 1988.

DURSTELER, M. R. AND WURTZ, R. H. Pursuit and optokinetic deficits following chemical lesions of cortical areas MT and MST. *J. Neurophysiol.* 60: 940–965, 1988.

FUCHS, A. F. AND MUSTARI, M. J. The optokinetic response in primates and its possible neuronal substrate. In: *Reviews of Oculomotor Research 5. Visual Motion and Its Role in the Stabilization of Gaze*, edited by F. A. Miles and J. Wallman. New York: Elsevier, 1993, p. 343–369.

GEORGOPOULOS, A. P. On reaching. *Annu. Rev. Neurosci.* 9: 147–170, 1986.

GOLDBERG, M. E. AND BRUCE, C. J. Primate frontal eye fields. III. Maintenance of a spatially accurate saccade signal. *J. Neurophysiol.* 64: 489–508, 1990.

GOLDBERG, M. E. AND SEGRAVES, M. A. The visual and frontal cortices. In: *The Neurobiology of Saccadic Eye Movements*, edited by R. H. Wurtz and M. E. Goldberg. New York: Elsevier, 1989, p. 283–314.

GOTTLIEB, J. P., BRUCE, C. J., AND MACAVOY, M. G. Smooth eye movements elicited by microstimulation in the primate frontal eye field. *J. Neurophysiol.* 69: 786–799, 1993.

GOTTLIEB, J. P., MACAVOY, M. G., AND BRUCE, C. J. Unit activity related to smooth pursuit eye movements in rhesus monkey frontal eye fields. *Soc. Neurosci. Abstr.* 15: 1203, 1989.

GOTTLIEB, J. P., MACAVOY, M. G., AND BRUCE, C. J. Smooth eye movements elicited from the monkey periarcuate area: topography and relation to single unit responses. *Soc. Neurosci. Abstr.* 17: 544, 1991.

GRASSE, K. L. AND LISBERGER, S. G. Analysis of a naturally occurring asymmetry in vertical smooth pursuit eye movements in a monkey. *J. Neurophysiol.* 67: 164–179, 1992.

HOLZMAN, P. S. Recent studies of psychophysiology in schizophrenia. *Schizophr. Bull.* 13: 49–75, 1987.

HUERTA, M. F., KRUBITZER, L. A., AND KAAS, J. H. Frontal eye field as defined by intracortical microstimulation in squirrel monkeys, owl monkeys, and macaque monkeys. I. Subcortical connections. *J. Comp. Neurol.* 253: 415–439, 1986.

HUERTA, M. F., KRUBITZER, L. A., AND KAAS, J. H. Frontal eye field as defined by intracortical microstimulation in squirrel monkeys, owl monkeys, and macaque monkeys. II. Cortical connections. *J. Comp. Neurol.* 265: 332–361, 1987.

JUDGE, S. J., RICHMOND, B. J., AND CHU, F. C. Implantation of magnetic search coils for measurement of eye position: an improved method. *Vision Res.* 20: 535–538, 1980.

KAWANO, K., SASAKI, M., AND YAMASHITA, M. Response properties of neurons in posterior parietal cortex of monkey during visual-vestibular stimulation. I. Visual tracking neurons. *J. Neurophysiol.* 51: 340–351, 1984.

KEATING, E. G. Frontal eye field lesions impair predictive and visually guided pursuit eye movements. *Exp. Brain Res.* 86: 311–323, 1991.

KEATING, E. G. Lesions of the frontal eye field impair pursuit eye movements, but preserve the predictions driving them. *Behav. Brain Res.* 53: 91–104, 1993.

KELLER, E. L. AND CRANDALL, W. F. Neuronal responses to optokinetic stimuli in pontine nuclei of behaving monkey. *J. Neurophysiol.* 49: 169–187, 1983.

KELLER, E. L. AND HEINEN, S. J. Generation of smooth-pursuit eye movements: neuronal mechanisms and pathways. *Neurosci. Res.* 11: 79–107, 1991.

KOMATSU, H. AND WURTZ, R. H. Relation of cortical areas MT and MST to pursuit eye movements. I. Localization and visual properties of neurons. *J. Neurophysiol.* 60: 580–603, 1988.

KOMATSU, H. AND WURTZ, R. H. Modulation of pursuit eye movements by stimulation of cortical areas MT and MST. *J. Neurophysiol.* 62: 31–47, 1989.

KRAUZLIS, R. J. AND LISBERGER, S. G. Visual motion commands for pursuit eye movements in the cerebellum. *Science Wash. DC* 253: 568–571, 1991.

LEICHNETZ, G. R. The frontal eye field projects to the nucleus prepositus hypoglossi in the monkey. *Neurosci. Lett.* 54: 185–188, 1985.

LEICHNETZ, G. R. Inferior frontal eye field projections to the pursuit-related dorsolateral pontine nucleus and middle temporal area in the monkey. *Vis. Neurosci.* 3: 171–180, 1989.

LEIGH, R. J. AND ZEE, D. S. *The Neurology of Eye Movements.* Philadelphia: Davis, 1991.

LEVIN, S. Frontal lobe dysfunctions in schizophrenia. I. Eye movement impairments. *J. Psychiat. Res.* 18: 27–55, 1984.

LEVY, D. L., HOLZMAN, P. S., MATTHYSSE, S., AND MENDELL, N. R. Eye tracking dysfunction and schizophrenia—a critical perspective. *Schizophr. Bull.* 19: 461–536, 1993.

LISBERGER, S. G. AND FUCHS, A. F. Role of primate flocculus during rapid behavioral modification of vestibulo-ocular reflex. I. Purkinje cell activity during visually guided horizontal smooth pursuit eye movements and passive head rotation. *J. Neurophysiol.* 41: 733–763, 1978.

LISBERGER, S. G., MORRIS, E. J., AND TYCHSEN, L. Visual motion processing and sensor-motor integration for smooth pursuit eye movements. *Annu. Rev. Neurosci.* 10: 97–130, 1987.

LYNCH, J. C. Frontal eye field lesions in monkeys disrupt visual pursuit. *Exp. Brain Res.* 68: 437–441, 1987.

LYNCH, J. C. Pursuit recovery after frontal eye field lesions in monkeys. *Soc. Neurosci. Abstr.* 15: 1202, 1989.

MACAVOY, M. G., GOTTLIEB, J. P., AND BRUCE, C. J. Smooth pursuit eye movement representation in the primate frontal eye field. *Cereb. Cortex* 1: 95–102, 1991.

MAY, J. G., KELLER, E. L., AND CRANDALL, W. F. Changes in eye velocity during smooth-pursuit tracking induced by microstimulation in the dorsolateral pontine nucleus of the monkey. *Soc. Neurosci. Abstr.* 11: 79, 1985.

MAY, J. G., KELLER, E. L., AND SUZUKI, D. A. Smooth-pursuit eye movement deficits with chemical lesions in the dorsolateral pontine nucleus of the monkey. *J. Neurophysiol.* 59: 952–977, 1988.

MILES, F. A. AND FULLER, J. H. Visual tracking and the primate flocculus. *Science Wash. DC* 189: 1000–1002, 1975.

MORROW, M. J. AND SHARPE, J. A. Cerebral hemispheric localization of smooth pursuit asymmetry. *Neurology* 40: 284–292, 1990.

MUSTARI, M. J., FUCHS, A. F., AND WALLMAN, J. Response properties of dorsolateral pontine units during smooth pursuit in the rhesus macaque. *J. Neurophysiol.* 60: 664–686, 1988.

NEWSOME, W. T., WURTZ, R. H., DURSTELER, M. R., AND MIKAMI, A. Deficits in visual motion processing following ibotenic acid lesions of the middle temporal visual area of the macaque monkey. *J. Neurosci.* 5: 825–840, 1985.

NEWSOME, W. T., WURTZ, R. H., AND KOMATSU, H. Relation of cortical areas MT and MST to pursuit eye movements. II. Differentiation of retinal from extraretinal inputs. *J. Neurophysiol.* 60: 604–620, 1988.

NODA, H. AND MIKAMI, A. Discharges of neurons in the dorsal parafloccullus of monkeys during eye movements and visual stimulation. *J. Neurophysiol.* 56: 1129–1146, 1986.

PIERROT-DESEILLIGNY, C. Saccade and smooth pursuit impairment after cerebral hemispheric lesions. *Eur. Neurol.* 34: 121–134, 1994.

RASHBASS, C. The relationship between saccadic and smooth tracking eye movements. *J. Physiol. Lond.* 159: 326–338, 1961.

ROBINSON, D. A. A method of measuring eye movements using a scleral search coil in a magnetic field. *IEEE Trans. Biomed. Eng.* 10: 137–145, 1963.

ROBINSON, D. A. AND FUCHS, A. F. Eye movements evoked by stimulation of frontal eye fields. *J. Neurophysiol.* 32: 637–648, 1969.

SCHALL, J. D. Neuronal activity related to visually guided saccadic eye movements in the frontal eye fields of rhesus monkeys: comparison with supplementary eye fields. *J. Neurophysiol.* 66: 559–579, 1991.

SEGRAVES, M. A. AND PARK, K. The relationship of monkey frontal eye field activity to saccade dynamics. *J. Neurophysiol.* 69: 1880–1889, 1993.

STANTON, G. B., BRUCE, C. J., AND GOLDBERG, M. E. Topography of projections to posterior cortical areas from the macaque frontal eye fields. *J. Comp. Neurol.* In press.

STANTON, G. B., GOLDBERG, M. E., AND BRUCE, C. J. Frontal eye field efferents in the macaque monkey. II. Topography of terminal fields in midbrain and pons. *J. Comp. Neurol.* 271: 493–506, 1988.

STONE, L. S. AND LISBERGER, S. G. Visual responses of Purkinje cells in the cerebellar flocculus during smooth-pursuit eye movements in monkeys. I. Simple spikes. *J. Neurophysiol.* 63: 1241–1261, 1990a.

STONE, L. S. AND LISBERGER, S. G. Visual responses of Purkinje cells in the cerebellar flocculus during smooth-pursuit eye movements in monkeys. II. Complex spikes. *J. Neurophysiol.* 63: 1262–1275, 1990b.

SUZUKI, D. A. AND KELLER, E. L. The role of the posterior vermis of

monkey cerebellum in smooth-pursuit eye movement control. I. Eye and head movement-related activity. *J. Neurophysiol.* 59: 1–18, 1988a.

SUZUKI, D. A. AND KELLER, E. L. The role of the posterior vermis of monkey cerebellum in smooth-pursuit eye movement control. II. Target velocity-related Purkinje cell activity. *J. Neurophysiol.* 59: 19–40, 1988b.

SUZUKI, D. A., MAY, J. G., KELLER, E. L., AND YEE, R. D. Visual response properties of neurons in the dorsolateral pontine nucleus of the alert monkey. *J. Neurophysiol.* 63: 37–69, 1990a.

SUZUKI, D. A., YEE, R. D., AND BETELAK, K. Deficits in smooth-pursuit eye movements following lidocaine injection in monkey nucleus reticularis tegmenti pontis (NRTP). *Soc. Neurosci. Abstr.* 16: 903, 1990b.

SUZUKI, D. A., YAMADA, T., BETELAK, K. F., AND YEE, R. D. Smooth-pursuit eye movement related activity in monkey nucleus reticularis tegmenti pontis. *Soc. Neurosci. Abstr.* 17: 459, 1991.

THIER, P. AND ERICKSON, R. G. Responses of visual-tracking neurons from cortical area MST-1 to visual, eye and head motion. *Eur. J. Neurosci.* 4: 539–553, 1992.

THIER, P., KOEHLER, W., AND BUETTNER, U. W. Investigation of the dorsolateral basilar pontine grey of the alert monkey. *Brain Behav. Evol.* 33: 75–79, 1989.

TUSA, R. J. AND UNGERLEIDER, L. G. Fiber pathways of cortical areas mediating smooth pursuit eye movements in monkeys. *Ann. Neurol.* 23: 174–183, 1988.

UNGERLEIDER, L. G. AND DESIMONE, R. Cortical connections of visual area MT in the macaque. *J. Comp. Neurol.* 248: 190–222, 1986.

WEINBERGER, D. R., BERMAN, K. F., AND ZEC, R. F. Physiological dysfunction of dorsolateral prefrontal cortex in schizophrenia. I. Regional cerebral blood flow (rCBF) evidence. *Arch. Gen. Psychiat.* 43: 114–124, 1986.